



## Development and application of a spatial stock assessment model for pāua (*Haliotis iris*)

New Zealand Fisheries Assessment Report 2020/30

P. Neubauer

ISSN 1179-5352 (online)

ISBN 978-1-99-004317-8 (online)

October 2020



Requests for further copies should be directed to:

Publications Logistics Officer  
Ministry for Primary Industries  
PO Box 2526  
WELLINGTON 6140

Email: [brand@mpi.govt.nz](mailto:brand@mpi.govt.nz)  
Telephone: 0800 00 83 33  
Facsimile: 04-894 0300

This publication is also available on the Ministry for Primary Industries websites at:  
<http://www.mpi.govt.nz/news-and-resources/publications>  
<http://fs.fish.govt.nz> go to Document library/Research reports

**© Crown Copyright - Fisheries New Zealand**

## TABLE OF CONTENTS

<b>EXECUTIVE SUMMARY</b>	<b>1</b>
<b>1 INTRODUCTION</b>	<b>2</b>
<b>2 METHODS</b>	<b>2</b>
2.1 Spatial model inputs . . . . .	2
2.1.1 Catch . . . . .	2
2.1.2 Catch-per-unit-effort . . . . .	5
2.1.3 Commercial length-frequency data . . . . .	5
2.2 Spatial assessment model . . . . .	7
2.2.1 Main population dynamics . . . . .	8
2.2.2 Data models . . . . .	10
2.2.3 Prior distributions . . . . .	11
2.2.4 Data weighting . . . . .	12
2.2.5 Technical model details . . . . .	13
2.3 Model comparisons . . . . .	13
<b>3 RESULTS</b>	<b>13</b>
3.1 Comparisons for PAU 5B . . . . .	13
3.2 Comparisons for PAU 5D . . . . .	13
<b>4 DISCUSSION</b>	<b>24</b>
<b>5 ACKNOWLEDGMENTS</b>	<b>25</b>
<b>6 REFERENCES</b>	<b>25</b>
<b>APPENDIX A SUPPLEMENTARY FIGURES</b>	<b>27</b>
<b>APPENDIX B PRIOR PREDICTIVE SIMULATIONS</b>	<b>30</b>
B.1 Uniform priors . . . . .	30
B.2 Informed priors . . . . .	30
<b>APPENDIX C MODEL COMPARISON</b>	<b>35</b>
C.1 PAU 5B . . . . .	35
C.2 PAU 5D . . . . .	39



## **EXECUTIVE SUMMARY**

**Neubauer, P. (2020). Development and application of a spatial stock assessment model for pāua (*Haliotis iris*).**

**New Zealand Fishery Assessment Report 2020/30. 42 p.**

A spatial assessment model for pāua (*Haliotis iris*) was developed to better incorporate the effect of demographic variability and spatial catch patterns on pāua population dynamics, and to facilitate spatial management procedure evaluation and implementation. The model was fitted to spatially-resolved input data and compared with single-area versions of the assessment models for pāua quota management areas PAU 5B and PAU 5D. These quota management areas (QMA), chosen as the respective assessment models, allowed a robust comparison based on different characteristics: the model for PAU 5B provides subjectively “good” estimates of model parameters and population trajectories and, therefore, provides a “best case” test, whereas the model for PAU 5D is sensitive to growth assumptions and model weighting, providing a more challenging test case.

The spatial model developed here provided qualitatively different inferences in each QMA compared with the single-area models. The spatial model performed well in technical terms for both QMAs in that it provided well-defined estimates for all model parameters. Nevertheless, it performed markedly differently to the single-area model in PAU 5D, but provided similar estimates to the single-area model in PAU 5B. In PAU 5D, the inferred catch history on the regional scale suggested that only a single area was affected by catch reductions in the mid-2000s, but all areas showed comparable increases in catch-per-unit-effort (CPUE) at this time. The spatial model did not attribute the increase in CPUE (and by extension, available biomass in the model) to the decreases in catch, but estimated a considerably higher biomass, and attributed the increase in CPUE (and available biomass in the model) to recruitment. As a result, the total biomass and stock status in the spatial model were estimated to be markedly higher than in the single-area model.

The spatial model provides an opportunity to incorporate spatial patterns in both fishing and demographics in the assessment and management of pāua. It provides complementary information to inferences made using the single-area model, and can be used to test the impact of spatial homogeneity assumptions in the single-area model.

## 1. INTRODUCTION

Demographic variability is a key feature of abalone population dynamics. For New Zealand blacklip abalone, pāua (*Haliotis iris*), growth is known to vary across different spatial scales, from tens of metres to hundreds of kilometres (McShane & Naylor 1995, Prince 2005, Naylor et al. 2006). On a New Zealand-wide scale, small-sized pāua are found in northern New Zealand, whereas large-size pāua are fished in southern waters off Stewart Island.

With the recent development of pāua data loggers (Abraham 2012, Neubauer et al. 2014), and electronic statutory reporting in the near future, near real-time information of fishery effort and catch is now available at a fine spatial scale. The development of global positioning system-(GPS)-logging technology followed from the realisation that pāua stocks are a mosaic of small stocks with limited connectivity by dispersal of pelagic eggs and larvae (McShane & Naylor 1995, McShane 1998, Prince 2005, Naylor et al. 2006). Among these sub-stocks, biological characteristics such as growth and size-at-maturity can vary substantially. As a result, recent assessments and management, conducted at the scale of Quota Management Areas (QMAs), do not reflect the variability in biological characteristics.

Providing and applying management advice over relatively large spatial scales can lead to patterns of local overexploitation of accessible stocks—i.e., the management scale does not match the scale of the fishery (Cope & Punt 2011). Depletion of local populations can, in turn, result in a number of undesirable outcomes: because pāua is an important species for customary and recreational fisheries, local governance conflicts may arise from local depletion or perceived overfishing by commercial fishers (e.g., popular recreational areas may receive disproportionate effort and deplete rapidly). The collapse of local sub-populations may also lead to slow rebuilding of the larger QMA-scale stock when recruitment is impaired due to the low density of spawners.

Recently, the availability of data from the pāua data-logger programme has led to the development of voluntary spatial management tools that are meant to overcome the potential of local depletion and associated conflicts. These tools include online dashboards that display in-season catch and standardised catch rates at a relatively small (i.e., statistical area) scale to fishers. These dashboards can be used to monitor local stocks and set empirical harvest procedures. Nevertheless, the effectiveness of spatial harvest procedures cannot be tested without a spatially explicit operating model. Management procedures have been developed and simulation-tested in pāua QMA 5 (Neubauer 2019), but have to date not included spatial aspects of the fishery due to limitations of the assessment model. Interactions with fishers have highlighted that this limitation is an important shortfall given the spatially complex nature of the fishery. Recent efforts to apply both local and regional (QMA-scale) management procedures highlight the need for a spatially explicit assessment and management tool that can be used to support spatially explicit management procedures.

This project developed a spatially explicit assessment model that can serve as an alternative operating model for assessment and management procedures, and allow managers and industry to address spatial management questions. The spatial assessment model takes advantage of spatially resolved catch and effort, catch-sampling length frequency and growth data, and provides a basis for simulation testing of spatial management procedures.

## 2. METHODS

### 2.1 Spatial model inputs

#### 2.1.1 Catch

Catch is a key input into any stock assessment because it is often the only information that determines the scale of the fishery and the link between fishing mortality and stock dynamics. For the spatial assessment developed here, catch information was considered to be a limiting factor because the spatial resolution of reported catch in pāua fisheries has increased over time, but assumptions needed to be made about the spatial distribution of early catches. These assumptions are generally necessary at almost any spatial

scale for pāua fisheries: for example, for PAU 5A, PAU 5B and PAU 5D, catches prior to 1996 were recorded on the spatial scale of research strata (Figures 1, 2), some of which straddle the boundaries of the more recent (1996) subdivision of PAU 5 into PAU 5A, B and D. As a result, early catch from these overlapping research strata cannot be unambiguously assigned to each QMA. There is no information available at smaller spatial scales than the research strata prior to 1996, and the currently used fine-scale statistical areas were only introduced with Paua Catch Effort and Landing Return (PCELRL) forms and record keeping in 2001.

Due to the limitations in the spatial resolution of early catch, the spatial resolution of research strata was chosen as an appropriate resolution for the current development of the spatial model (Figures 1, 2). Because the influence of data from early fishing will diminish over time, it may be feasible to fit the model to relatively fine spatial data in the near future. Nevertheless, as a proof of concept, the current model was kept relatively simple.

The terms “area” or “region” are used as general terms for sub-stocks that make up the overall stock in the spatial assessment—these terms both refer to research strata throughout. Although these areas are generally referred to with a zero preceding the research stratum code (or Landing Area in the data; Figures 1, 2), the zeros were subsequently omitted from the code for convenience; for example, area (or region) 25 indicates data from Landing Area 025.

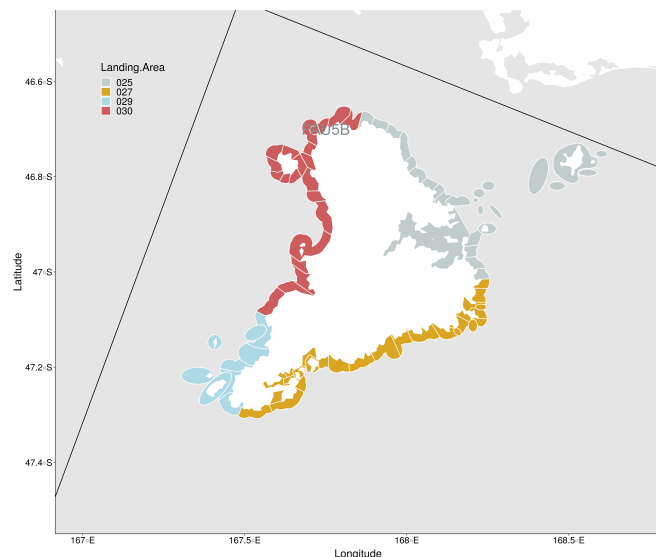


**Figure 1: Map of fine-scale statistical areas (coloured polygons delimited by white lines) for pāua management area PAU 5B, coloured by research strata (Landing\_Area), the highest spatial resolution for the recording of catch-per-unit-effort prior to 1996. Fine-scale areas as mapped have been used since 2001 (intermediate-resolution strata were in use between 1996 and 2001).**

At the QMA level, the same assumptions were made as in previous assessments about the attribution of total catch to research strata (Marsh & Fu 2017, Neubauer & Tremblay-Boyer 2019b), in part to ensure comparable results between the spatial and non-spatial models. The method consists of using the reported Catch Effort and Landing Return (CELR) data to attribute total catch. These assumptions have not been reviewed for some time, and should probably be re-examined to ensure continued support for the methods.

At the regional scale (research stratum level), the following assumptions were made: in view of the uncertain early catch history, catch was assumed to be constant at 148 t for PAU 5D and 250 t for PAU 5B from 1984–1995. Prior to 1984, the increase of the fishery was assumed to be linear from zero catch in 1964. The reported catch split from CELR data from the 1984–1995 period was used to allocate total catch to regions for this period (CELR reporting was largely incomplete in these years, so could not be used to estimate total catch by region). The same regional catch proportions were used to assign catch

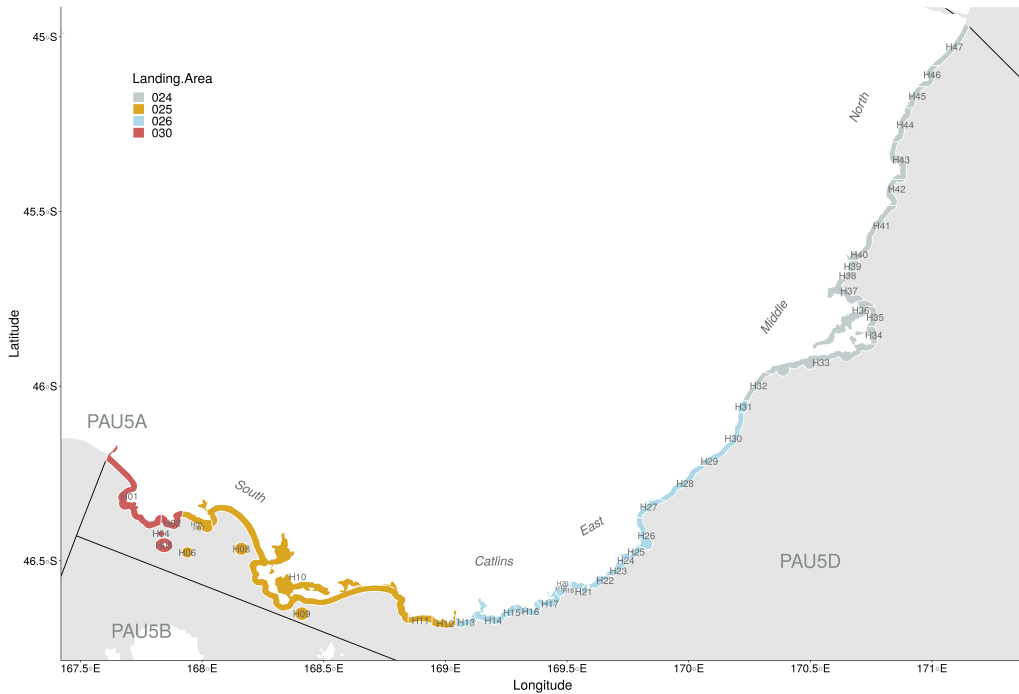


**Figure 2:** Map of fine-scale statistical areas (coloured polygons delimited by white lines) for pāua management area PAU 5D, coloured by research strata (Landing\_Area), the highest spatial resolution for the recording of catch-per-unit effort prior to 1996. Fine-scale areas as mapped have been used since 2001 (intermediate resolution strata were in use between 1996 and 2001).

prior to 1984 to regions. From 1996 onward, regionally reported CELR and PCELR catch data were used (the estimated catch history is shown in Figure 3).

In PAU 5B, three of the four areas provided large catches. There were reasonable reductions in catches since the early 2000s, with reductions largely proportional to early catch: areas with higher catch also showed greater reductions. Catches from the three larger areas (25, 27 and 30) remained on a similar scale through most of the 2000s. The only area with no reduction in catch was the small area 29.

For PAU 5D, much of the early catch is attributed to research stratum 26 (the Catlins region), which correlates with anecdotal accounts from the fishery. Nevertheless, as catch was reduced in the early and mid-2000s, this reduction primarily affected the Catlins region, with markedly smaller, if any, reductions in catch in other areas.

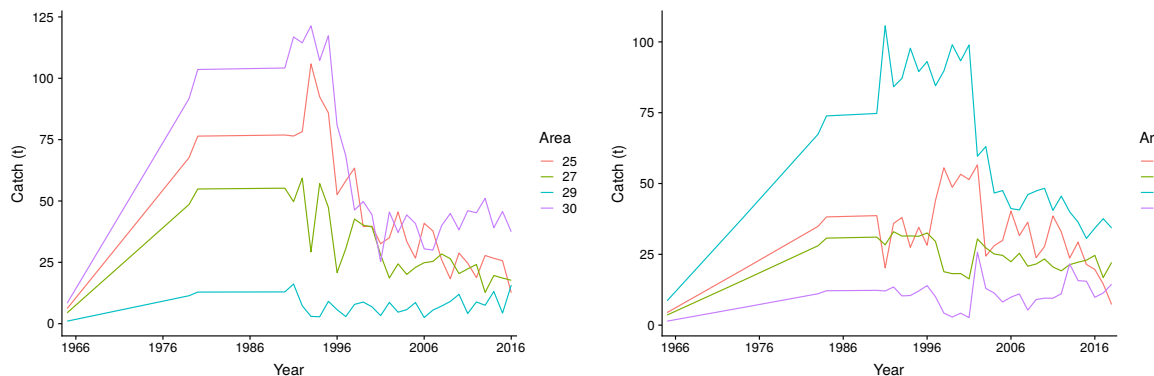


**Figure 3:** Assumed regional catch history for pāua management areas PAU 5B (left panel) and PAU 5D (right panel) by research strata (areas).

Assumptions for recreational and customary catch were identical to past assessments (Marsh & Fu 2017, Neubauer & Tremblay-Boyer 2019b), with partitioning to regions according to the commercial catch split. Although this assumption is likely to be incorrect for PAU 5D (the sparsely-populated Catlins region with a probable low recreational take), it is unlikely to have a marked effect on the model owing to the small scale of these catch components.

### 2.1.2 Catch-per-unit-effort

Catch-per-unit-effort (CPUE) indices for each region were generated in the same way as for the single-area assessment for PAU 5D (Neubauer & Tremblay-Boyer 2019a). Here, a region-year random effect was added to ensure that a region-specific trend could be extracted. Fits were similar to single-area fits, because the region-year effect itself was small for both areas (Figures 4, 5).

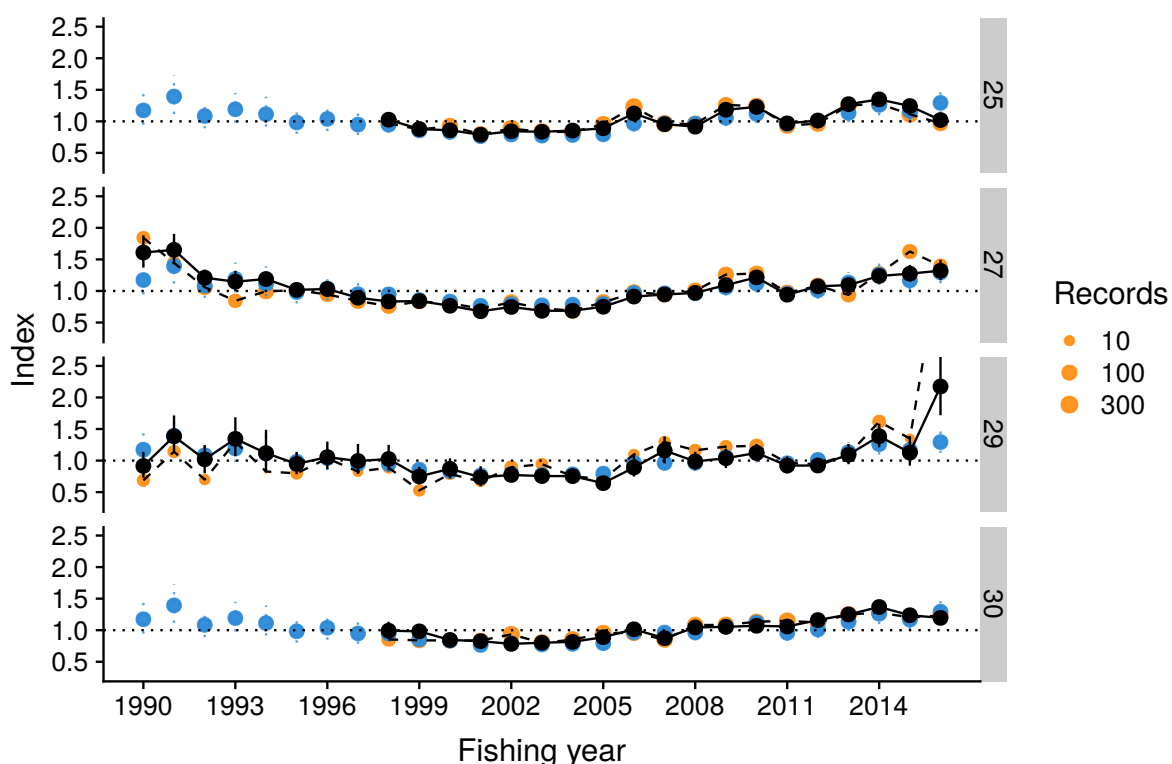


**Figure 4:** Standardisation of catch-per-unit-effort (CPUE) data using the generalised linear mixed model for combined Catch Effort Landing Return and Paua Catch Effort Landing Return data for pāua management area PAU 5B. Shown are the un-standardised geometric mean CPUE (orange dots and dashed line) with transparency scaled by the number of records, the year effects across all areas (blue with 95% confidence interval as dashed vertical lines) and the region-specific trend (black circles with 95% confidence interval).

### 2.1.3 Commercial length-frequency data

The most recent PAU 5D stock assessment used a Dirichlet Multinomial (DM) model to adjust observation error variance in commercial catch length-frequency (LF) data (Neubauer & Tremblay-Boyer 2019b). This method extended methods proposed by Thorson (2014) by accounting for sources of spatial variability, and adjusting the DM concentration parameter based on attributes of the data (e.g., the statistical area that samples came from). Although this method adjusted variability, it did not adjust the length frequencies and, therefore, assumed that the sampled length frequencies were representative of length frequencies at the population level. Here, the model was extended to a standardisation model that adjusts the length-frequency samples based on spatial and temporal variability. This adjustment is

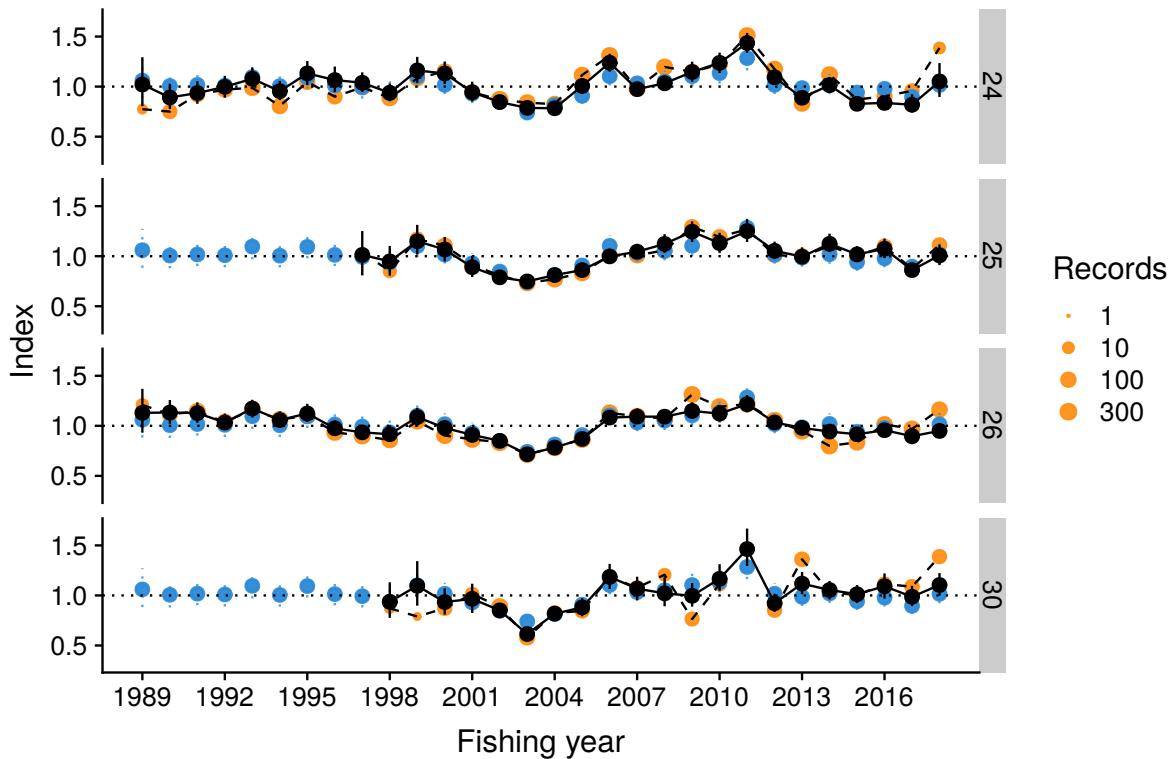


**Figure 5:** Standardisation of catch-per-unit-effort (CPUE) data using the generalised linear mixed model for combined Catch Effort Landing Return and Paua Catch Effort Landing Return data for pāua management area PAU 5D. Shown are the un-standardised geometric mean CPUE (orange dots and dashed line) with transparency scaled by the number of records, the year effects across all areas (blue with 95% confidence interval as dashed vertical lines) and the region-specific trend (black circles with 95% confidence interval).

similar to adjustments in CPUE applied during the standardisation of CPUE. This procedure has the advantage that reasonably smooth length-frequency distributions (i.e., filtering out variability from highly multi-modal LF distributions that arise due to low sample numbers) for sparsely sampled strata can be extracted, even if individual samples in those strata are unlikely to provide a reliable estimate of the true length frequencies of those strata.

The model setup was as follows, starting with the assumption that for every year  $y$ , there is a true stock-level composition  $\pi$  of numbers-at-length. Nevertheless, there is spatial variability in the composition so that in any particular region (research stratum)  $r$  and year  $y$ , there is a true composition  $\hat{\pi}_{y,r}$ , from which  $n_{y,r,s}$  pāua are sampled from statistical area  $s$ , giving a sample  $\{\pi_{y,r,s}, n_{y,r,s}\}$ . It was further assumed that the  $\pi_{y,r,s}$  are distributed according to a Dirichlet Multinomial distribution (DMN) with parameters  $\beta$  and  $\hat{\pi}$ , meaning they are random samples of the true stock-level proportions  $\pi$  with  $\beta$ , a concentration parameter. This parameter  $\beta$  can be considered a sample size in a Bayesian context, and is inversely proportional to the variance.

A crucial assumption is that the true compositions  $\hat{\pi}_{y,r,s}$  are, on the centered-log ratio scale, determined by mean proportions  $\Pi$  and random deviations for year ( $\omega_y$ ), region ( $\omega_r$ ) and statistical area ( $\omega_s$ ). The multivariate effects were estimated on a unit-(multi)normal scale with correlation matrix  $\Sigma$  and subsequently scaled by the corresponding random effects standard deviations  $\sigma$ . The overall scale of these deviations was estimated from a hyper-parameter  $\sigma_{sd}$ . This approach led to a model that effectively attributed variability in length-frequency data to spatial and temporal variability while accounting for the compositional (i.e., non-independent, constrained) nature of the data. The model for observation  $i$  in region  $r$  and statistical areas  $s$  can then be written as:

$$\pi_{y,r,s} \sim DMN(n_i, \hat{pi}_{y,r,s}, \beta), \quad (1)$$

$$\hat{pi}_{y,r,s} = C(\Pi + \sigma_y \omega_y + \sigma_r \omega_r + \sigma_{ry} \omega_{ry} + \sigma_r \omega_r + \sigma_s \omega_s), \quad (2)$$

$$\omega_i \sim MVN(0, \Sigma_i), \quad (3)$$

$$\Sigma \sim LKJ(1), \quad (4)$$

$$\sigma_i \sim N(0, \sigma_{sd}), \quad (5)$$

$$\sigma_{sd} \sim N(0, P). \quad (6)$$

The LKJ distribution is a prior probability distribution on correlation matrices, MVN is the multivariate normal distribution, N is the normal distribution and P is a prior on the standard deviation of the random effects scale for random effects  $i \in [r, y, s, ry]$ , where  $ry$  is the deviation in region  $r$  for year  $y$ . The DM model was implemented in Stan (Stan Development Team 2018) and parameters were estimated across all length-frequency data for the period 2001–2017. Earlier data were considered too sparse to use in the model. The estimation used Stan’s No U-turn sampler for full Markov chain Monte Carlo (MCMC) estimation of all model parameters.

The DM model converged well for both PAU 5B and PAU 5D (see Figure A-1 for an example of diagnostics for PAU 5B, results were almost identical for PAU 5D) and produced similar outputs for both management areas. The outputs suggested that spatial variation at the statistical-area level contributed significantly to between-sample variation in proportion-at-length data in both QMAs (see Figures A-2, A-3 for an example of outputs for PAU 5D, results were almost identical for PAU 5B).

For both QMAs and for all regions, the posterior distribution of the length frequencies included the sampled length frequencies for region-year combinations with a large number of landings and sampled pāua (Figures 6,7). For areas and years with few or no samples, the model could use information from other years and regions to construct a likely length-frequency distribution, albeit with large error bars for these strata. Because the error from this procedure is directly included in the assessment as observation error, this uncertainty is considered to be adequately represented.

Estimated posterior length-proportions for each region and year were extracted from the model as the posterior mean of the clr-(centered log-ratio)-transformed proportions ( $\pi_{r,y}$ ) for use in the stock assessment. The clr-transform is defined as  $clr(\pi) = \log(\pi) - \overline{\log(\pi)}$ , with its inverse defined as  $clr^{-1}(x) = \text{clo}(\exp(x))$ , where clo is the closure (sum-to-one) operation. The posterior co-variance estimated from clr-transformed yearly proportions from MCMC draws was used as an estimate of observation error for clr-transformed proportions data in the final stock assessment model.

## 2.2 Spatial assessment model

Spatial assessment tools have been developed for a range of stocks in New Zealand and worldwide (e.g., Cadrian et al. 2019, Punt 2019b). The most common spatial assessment tools are tag-integrated models that account for movement between sub-stocks in large-scale fisheries (Goethel et al. 2011, Cadrian et al. 2019). For relatively immobile invertebrates such as abalone, however, there is limited adult movement between sub-stocks, and stock mixing is considered to occur mainly at the larval stage. For these species, sub-stocks are often assessed using independent models, or models that share parameters *a priori* (e.g., common recruitment patterns, catchability, natural mortality; Punt 2019b). The latter assessment models make strong assumptions about the similarity of demographic parameters for sub-stocks, but have the advantage that shared parameters can be estimated from multiple datasets, which may improve convergence and estimation.

Statistically, these two strategies lie at opposing ends of a spectrum between pooled effects (shared parameters) and independent, fixed effects (independent assessments; Gelman & Hill 2006). Here, a model was set up that shared data of natural mortality, steepness and process error estimates among regions, but allowed for regionally-varying growth, maturation, selectivity and recruitment. In the first instance,

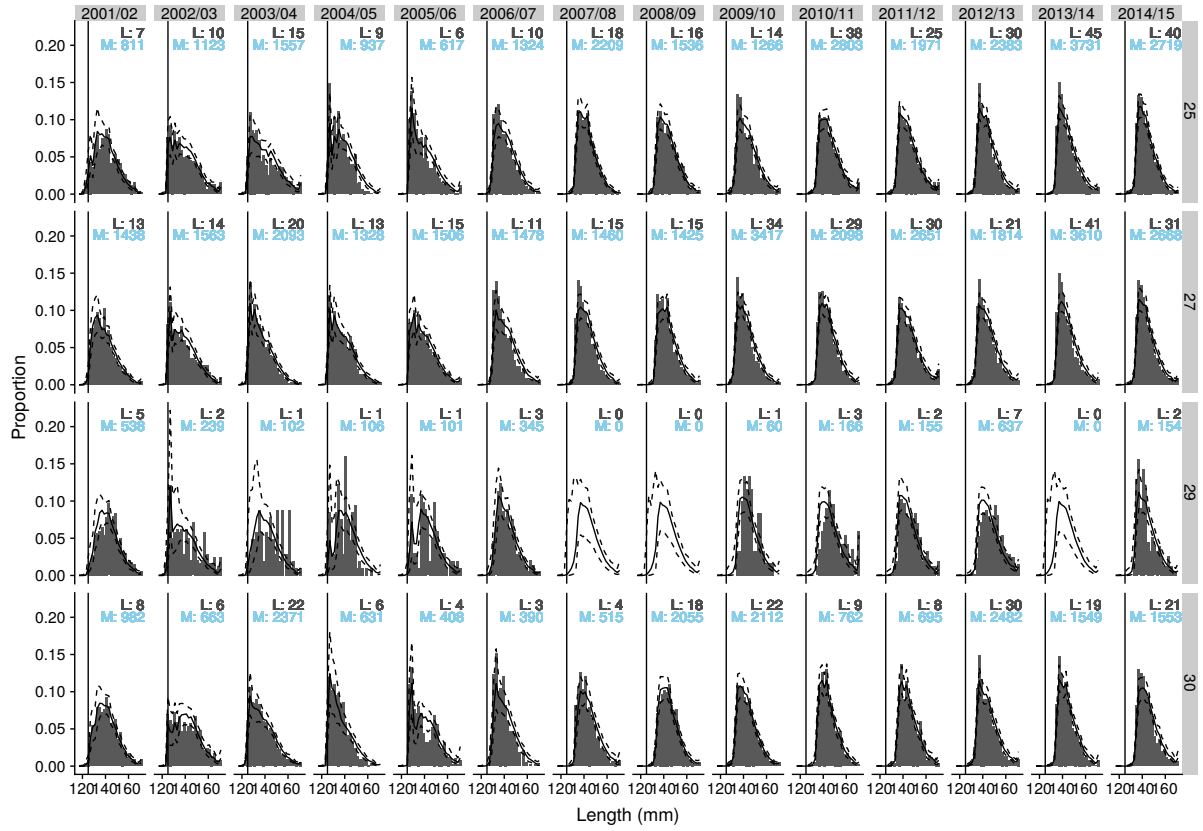


**Figure 6: Dirichlet-Multinomial posterior distributions for yearly proportions  $\pi_{r,y}$  (black line) in each of four regions in pāua management area PAU 5B, with 95% confidence intervals (dashed line). Raw catch sampling length frequency proportions are in grey; number of landings (L) in black; number of measurements (M) in blue.**

fully-shared or region-specific parameters were chosen, but the model implementation would allow the application of random effects to estimate region-specific parameters at smaller spatial scales. This aspect would enable the sharing of information among regions while allowing for some dissimilarity. Nevertheless, this latter model structure is difficult to implement with a small number of spatial strata like the research strata used here, because the random-effects variance cannot be reliably estimated with few strata.

### 2.2.1 Main population dynamics

Within each spatial area, the spatial assessment model employed the same dynamics as those described by Neubauer & Tremblay-Boyer (2019b). These dynamics were based on the model described by Breen et al. (2003): population dynamics in each spatial region (research stratum)  $r$  are written as beginning-of-year values  $N_r$  at length  $l$ , with  $l \in [1, L]$  in year  $y$  as:

$$N_{r,y} = (SN_{r,y-1} \circ SF_{r,y-1})G_r + R_{r,y}, \quad (7)$$

where  $N_{r,y}$  is used to denote the vector of numbers-at-lengths 1... $L$  (i.e., omitting the subscript denotes a vector);  $S = \exp(-M)$  is (region-independent) survival from natural mortality,  $SF_{r,y-1}$  is the length-specific survival after fishing ( $\circ$  is the element-wise multiplication),  $G_r$  is a  $L \times L$  growth-transition matrix for region  $r$ , and  $R_r$  is recruitment, which is evenly distributed among the first five length classes in the model. Element  $G_{r,i,j}$  of  $G_r$  is then the proportion of pāua transitioning from length class  $i$  to length class  $j$  in a given year in region  $r$ .

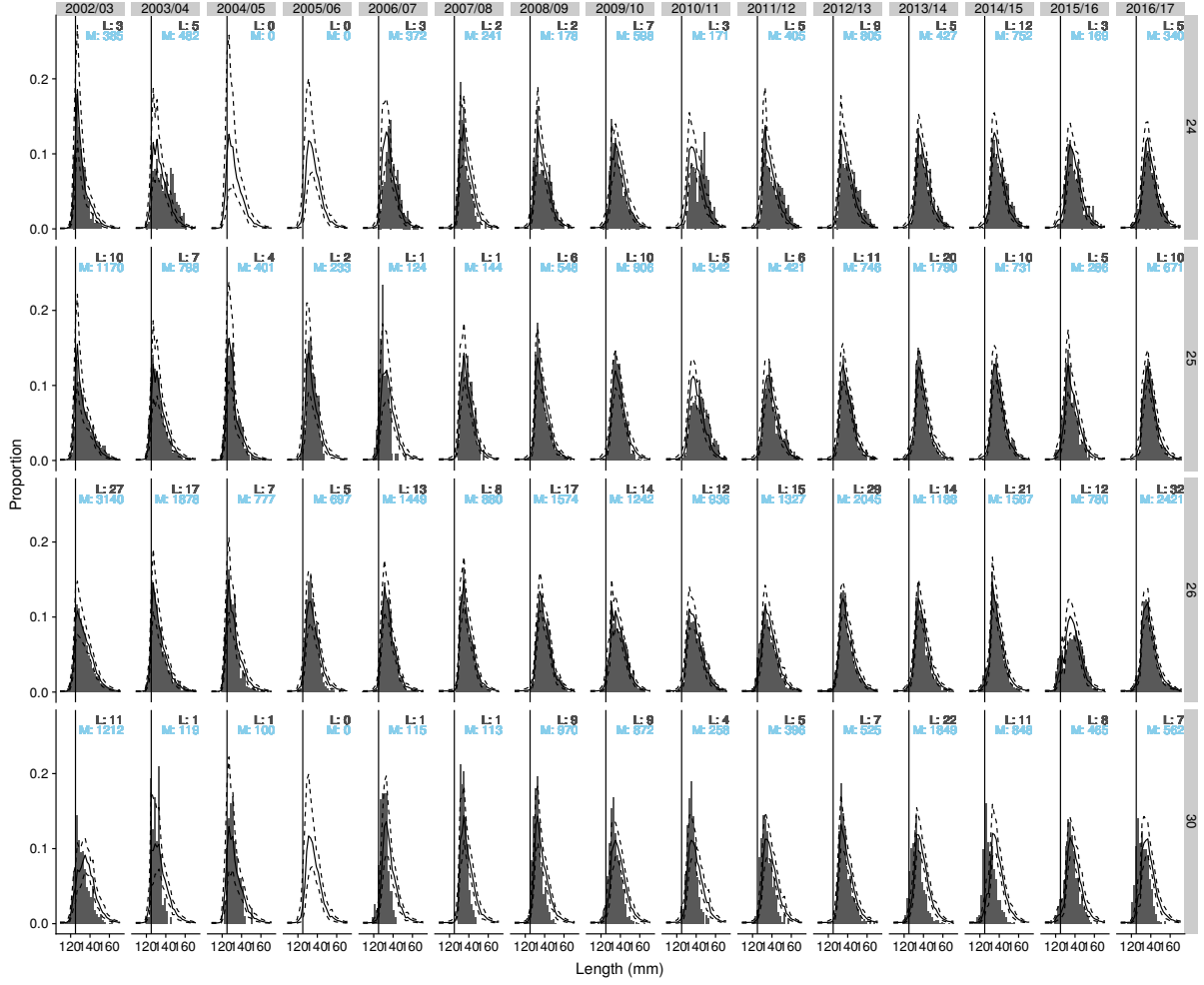


**Figure 7: Dirichlet-Multinomial posterior distributions for yearly proportions  $\pi_{r,y}$  (black line) in each of four regions in pāua management area PAU 5D, with 95% confidence intervals (dashed line). Raw catch sampling length frequency proportions are in grey; number of landings (L) in black; number of measurements (M) in blue.**

Survival  $S$  is derived from  $M$ , an estimated parameter in the model. Survival from fishing,  $SF_{r,y}$ , is calculated by applying region-specific selectivity  $V_{r,y}$  in year  $y$  to the overall exploitation rate  $U_{r,y}$  so that  $SF_{r,y} = 1 - U_{r,y}V_{r,y}$ , with  $U_{r,y}$  the regional ratio of catch  $TC_{r,y}$  in year  $y$  to available biomass  $B_{r,y}^{\text{avail}}$ , or  $U_{r,y} = TC_{r,y}/B_{r,y}^{\text{avail}}$ . Biomass is obtained by multiplying numbers-at-length  $N_{r,y}$  by a vector  $w$  of weight-at-length.

Selectivity was assumed to be logistic. The logistic selectivity describes a smooth increase in selectivity that is symmetric about the size at 50% selectivity ( $D^{50}$ ). With  $D^{50}$  and size at 95% selectivity ( $D^{50} + D^{95}$ ), selectivity was estimated for each region  $r$  using

$$V_{r,y,l} = \frac{1}{1 + \exp\left(\frac{-\log(19)(l - D_r^{50} + D^a D^s)}{D_r^{95}}\right)}, \quad (8)$$

where  $D^s$  is a specified offset from the baseline selectivity, reflecting voluntary increases in minimum harvest size (MHS), and  $D^a$  is an estimated parameter that accounts for only partial implementation of increased MHS across a QMA (e.g., only some statistical areas will be fished at higher MHS).

Recruitment  $R_{r,y}$  was assumed to follow a Beverton-Holt stock-recruit relationship whereby steepness  $h$  was invariant among regions, equilibrium recruitment  $R_0$  was estimated across all regions (for comparability with the single-area assessment), and regional unfished recruitment was estimated as  $R_r = \lambda_r R_0$  and  $\lambda_r$ , the proportion of the total recruitment that is attributed to region  $r$  (e.g., Punt 2019a). Assuming local stock-recruit relationships, regional annual recruitment deviations  $R_{r,\text{dev}}$  determine recruitment from the regions spawning stock biomass (SSB <sub>$r$</sub> ). The latter was determined from the weight-at-length relationship  $w$  and the proportion of mature pāua at length  $y$ , which was estimated using a prior derived from the growth-maturity model; it was adjusted in the model via estimated growth and its correlation with maturity (see Neubauer & Tremblay-Boyer 2019a for details).

Growth,  $G_r$ , was calculated from the estimated mean growth in region  $r$ , growth variability (standard deviation), and the proportion  $p_{r,l}$  of the population in region  $r$  that does not grow at any length  $l$ . Growth  $G_r$  is then (omitting the regional subscript for simplicity):

$$G_{i,i} = p_i + (1 - p_i) \int_0^{i+k/2} \text{CLN}(\mu_i, \sigma_i), \quad (9)$$

$$G_{i,j} = (1 - p_i) \int_{i-k/2}^{i+k/2} \text{CLN}(\mu_i, \sigma_i) \quad \text{for } j = i+1, L-1, \quad (10)$$

$$G_{i,L} = (1 - p_i)(1 - \int_0^{L-k/2} \text{CLN}(\mu_i, \sigma_i)), \quad (11)$$

where  $\text{CLN}(\mu_i, \sigma_i)$  is the cumulative distribution function of the log-normal distribution with mean  $\mu$  and standard deviation  $\sigma$  on the log-scale.

## 2.2.2 Data models

The assessment model was fitted to three main data sources: the CPUE index, length-frequency distributions derived from commercial catch sampling, and growth and maturity priors developed from tag-recapture and maturation sampling programmes.

The CPUE index was included on the log-scale and modelled as a normally-distributed variable with:

$$\text{CPUE}_{r,y} \sim N\left(\text{CPUE}_{r,y}^M, \sqrt{\text{OE}_{\text{CPUE},y}^2 + \text{PE}_{\text{CPUE}}^2}\right), \quad (12)$$

with  $\text{PE}_{\text{CPUE}}$ , the CPUE process error;  $\text{CPUE}_{r,y}^M$ , the model-predicted CPUE in year  $y$  and region  $r$ , calculated as the log of the proportion  $q$  of the available biomass in year  $y$   $B_{r,y}^{\text{avail}} = (V_{r,y} \circ N_{r,y})w$ , i.e.,  $\text{CPUE}_{r,y}^M = \log(q) + \log(B_{r,y}^{\text{avail}}) * \beta$ , with log catchability  $\log(q)$  treated as a “nuisance” parameter (i.e., it was not of immediate interest). The parameter  $\beta$  modulates the relation between CPUE and available biomass, and introduces hyper-stability for  $\beta < 1$ .

The spatial assessment model used the yearly-estimated error from the Bayesian CPUE standardisation as  $\text{OE}_{\text{CPUE}}$ , which led to more uncertain CPUE early in the time series (e.g., CELR data, especially year 1), and increased precision in later years (cf. figure 13 in Neubauer & Tremblay-Boyer 2019a).

Analogous to CPUE inputs, yearly catch sampling length frequency (CSLF) proportions at length were included as the mean of clr-transformed estimated mean proportions from the Dirichlet-multinomial standardisation model for raw CSLF data. The model derived estimated length frequencies for each year with associated error, which was considered to be the observation error for CSLF data (analogous to the OE for uncertainty in the CPUE index). The clr-transformation changed the data from an  $L$ -dimensional simplex (i.e.,  $\sum_{i=1}^L p_{y,i} = 1$ ) to an unconstrained  $L$ -dimensional space. The observed mean CSLF values

for year  $y$  are thus specified as multivariate-normal (MVN) distributed with uncertainty, and correlations specified by a  $L \times L$  dimensional covariance matrix of observation error  $\text{OE}_{\text{CSLF}_{r,y}}$ . Due to the strong correlations (positive and negative), a multiplicative process error formulation was used, giving:

$$\text{clr}(\text{CSLF}_{r,y}) \sim \text{MVN}\left(\text{CSLF}_{r,y}^M, (1 + \text{PE}_{\text{CSLF}_{r,y}})\text{OE}_{\text{CSLF}_{r,y}}\right), \quad \text{with} \quad (13)$$

$$\text{CSLF}_{r,y}^M = \text{clr}((V_{r,y} \circ N_{r,y})U_{r,y}), \quad (14)$$

where  $\text{clr}((V_{r,y} \circ N_{r,y})U_{r,y})$  are the clr-transformed predicted selected proportions at length in the model, and  $\text{PE}_{\text{clr}(\text{CSLF}_{r,y})} > 0$  the process error that is additional to OE.

The spatial assessment model was exclusively fitted to model outputs from pre-processing models on the input data. This approach was mainly taken for computational convenience; for example, the growth-maturation model takes considerable time to fit growth and length-at-maturity data for pāua, given long-range correlations in the model, the explicit solving of the differential equation for growth and the expansion of the dataset to include measurements across all QMAs.

Instead of fitting the model to growth data, relatively uninformative joint prior distributions were specified for the following: mean (log-scale) growth increments  $\mu = \mu_1, \dots, \mu_L$ , the log of the (log-scale) growth standard deviations  $\sigma = \sigma_1, \dots, \sigma_L$ , the logit of the proportions  $z$  of the total population that exhibits zero growth at each length class, and the logit of the proportions of the total population that are mature in each length class ( $y$ ). The prior was identical for growth in each region. The functional form of the relationship between elements of  $\mu, \sigma, z$ , and  $y$  is determined by an overall covariance matrix that encodes correlations both within and between these variables:

$$\langle \mu, \sigma, z, y \rangle \sim \text{MVN}(\overline{\langle \tilde{\mu}, \tilde{\sigma}, \tilde{z}, \tilde{y} \rangle}, \text{cov}(\langle \tilde{\mu}, \tilde{\sigma}, \tilde{z}, \tilde{y} \rangle)), \quad (15)$$

where the tilde designates samples from the posterior distribution of the growth-maturation model.

### 2.2.3 Prior distributions

The CPUE process error was estimated in the model using a half-normal prior distribution ( $N^0$ ), with prior standard deviation  $\tau_{\text{PE}_{\text{CPUE}}}$ :

$$\text{PE}_{\text{CPUE}} \sim N^0(\tau_{\text{PE}_{\text{CPUE}}}).$$

Similarly, the CSLF process error was estimated in the model using a half-normal prior distribution, with prior standard deviation  $\tau_{\text{PE}_{\text{CPUE}}}$ .

Recruitment deviations ( $R_{\text{dev}}$ ), equilibrium recruitment ( $R_0$ ), natural mortality ( $M$ ) and ( $\log(q)$ ),  $D_{50}$  and  $D_{95}$  were assigned log-normal priors, parameterised in terms of mean and standard deviation (sd; on the log-scale), with the sample mean for  $R_{\text{dev}}$  forced to one.

Steepness  $h$  was estimated in this iteration of the assessment model; it was assigned a beta distribution prior with parameters  $a$  and  $b$ , with  $a = 10$  and  $b = 4$  the default prior, leading to a wide prior that put most of the weight at  $h > 0.5$  (see Table 1 for other default priors).

Prior predictive simulations were used to assess the impact of different formulations of priors for  $R_0$  and  $\lambda$  for final stock status and maximum depletion. The procedure is similar to stochastic stock-reduction analysis (Walters et al. 2006) and proceeds as follows:

1. Draw N values from prior for all parameters (especially  $R_0$  and  $p$ ).

2. Simulate trajectories using same length-based dynamics used in stock assessment, removing observed catches for each region and year.
3. Compare parameter space where available biomass  $>0$  for all years with prior, discard any prior values where available biomass is below zero, retain  $n$  trajectories simulated from the reduced prior.
4. Inspect implied stock status and maximum depletion for all  $n$  retained draws.

**Table 1: Default priors used both the single-area and spatial pāua stock assessment models (LN=Lognormal, N=Normal, N<sup>0</sup>=half-normal), with prior standard deviation (SD) shown on the log-scale and on the positive scale (CPUE, catch-per-unit-effort; CSLF, catch sampling length frequency).**

Parameter	Symbol	Prior	Mean	SD	SD (pos)
Equilibrium recruitment	$R_0$	LN	13.5	0.5	$4.4 \times 10^5$
Recruitment deviations	$R_{\text{dev}}$	LN	0	2	54.1
Natural mortality	$M$	LN	log(0.12)	0.2	0.02
Length at 50% selectivity	$D_{50}$	LN	log(123)	0.03	3.69
95% selectivity offset	$D_{95}$	LN	log(5)	0.5	3.02
Selectivity increase	$D_a$	LN	0	1	2.16
Steepness	$h$	Beta	0.71	0.12	
CPUE process error	PE <sub>CPUE</sub>	N <sup>0</sup> (0.05)	0.04	0.03	
CSLF process error	PE <sub>CSLF</sub>	N <sup>0</sup> (2)	0.80	0.6	

An overly vague prior for either  $R_0$  and/or  $\lambda$  implies a strong prior on current stock status and maximum depletion: at high values for  $R_0$  and/or  $\lambda$ , the resulting scale of the biomass is that fishing has no impact—the prior strongly favours a stock status that reflects no fishing impact (Appendix B, Figure B-4). In contrast, small values for  $R_0$  and/or  $\lambda$  will lead to the rapid depletion of regional stocks in prior simulations, and these values are thus discarded (see Appendix B, Figure B-4).

Although the prior for  $R_0$  can be adjusted empirically from the above procedure, a suitable prior for  $\lambda$  can be determined by assuming that the scale of the fishery in each region is approximated by the relative catch in each area. This assumption is reflected in a prior by taking the mean catch proportion and the covariance of regional catch proportions on clr-transformed proportions as the prior for  $\lambda$  (Figure B-5). The full prior for regional recruitment then becomes:

$$\text{clr}(\lambda) \sim MVN(\overline{\text{clr}(p_{\text{Catch}})}, \text{cov}(\text{clr}(p_{\text{Catch}}))), \quad (16)$$

$$R_0 = LN(13.5, 0.5), \quad (17)$$

$$R_r = \lambda_r \cdot R_0. \quad (18)$$

## 2.2.4 Data weighting

In this assessment, the Kullback-Leibler divergence (KLD) was used as a method for data weighting via a measure of information loss. The method relies on the premise that there should be no *a priori* preference for any one dataset, and that relative weight should emerge as part of the analysis and model refinement process. In addition, it makes use of the total distribution for the compositional data rather than just the first moment (e.g., mean length) (for further detail see Neubauer & Tremblay-Boyer 2019b).

## 2.2.5 Technical model details

The model was initialised for a period of 60 years with constant recruitment at  $R_0$  and no fishing. All MCMC algorithms were run using the no-u-turn-sampler (NUTS) implemented in Stan. The Stan language is more efficient than conventional Metropolis Hastings or Gibbs sampling for MCMC, and also provides diagnostics that can signal biased MCMC transitions (divergences) and potential bias in estimated quantities from these transitions. All MCMC chains were, therefore, monitored for divergent transitions to ensure that MCMCs were not biased. Eight independent chains were run over 1000 iterations, with the first 500 samples discarded for each chain, and a further 2000 samples saved for inference and post-processing.

## 2.3 Model comparisons

The spatial model was compared with the single-area model for QMAs PAU 5B and 5D, with a focus on both similarity of outcomes and also differences and potential bias in the non-spatial assessments due to spatial dynamics. Comparisons were mainly at a qualitative level, with comparisons of overall fits and combined biomass trends in the spatial models relative to the single-area models: the aim here was not to compare numerical outcomes but to compare qualitative model behaviour and consequences for stock status estimates.

## 3. RESULTS

The spatial model converged and performed similarly to the single-area model in technical terms: all parameters could be estimated (see Appendix C, Figures C-8, C-9, C-12, C-13), although for some parameters (e.g., steepness, M), there was little information in the data to constrain those parameters beyond the prior constraints. Nevertheless, these parameters were estimated to propagate uncertainty about them to the final biomass estimates.

### 3.1 Comparisons for PAU 5B

As for previous assessments (e.g., Fu 2014), the single-area assessment for PAU 5B fitted the large decline and subsequent recovery in CPUE (Figure 8) with a corresponding trend in biomass (Figures 9, 10). These patterns were replicated in the spatial model (Figures 9 to 11); however, it was also evident from this model that not all of the pre-1996 research strata reached similar depletion levels in the early 2000s; the stock in research stratum 25 remained near 40% of  $SSB_0$  at the time, whereas other stocks in areas 27 and 29 were likely close to the soft limit of 20% of  $SSB_0$ . These differences were partly due to differences in estimated growth among regions: the stock in region 25 (i.e., the Foveaux Strait coast of Stewart Island) was estimated to grow more slowly than other regional stocks at Stewart Island (Figure 12). This slow growth commonly leads to higher estimated biomass because less of the biomass is available to the fishery (Neubauer & Tremblay-Boyer 2019b). Overall, however, both the single- and multi-area models showed increased growth relative to the prior.

The spatial model also provided insight into regional recruitment dynamics at Stewart Island, evident in synchronous recruitment patterns estimated for areas 25 and 30 (Foveaux Strait coast of Stewart Island) and areas 27 and 29, on the southern (east and west, respectively) side of Stewart Island (Figure 13). For the latter two areas, the synchrony was mainly evident in more recent years (i.e., since the late 1990s), with large year classes estimated between 2008 and 2010 to fit the increase in CPUE since 2011.

### 3.2 Comparisons for PAU 5D

Although the spatial assessments provided complementary information to the single-area assessment for the fishery in PAU 5B, the spatial assessment in PAU 5D diverged markedly from the single-area assessment outputs (Figures 14, 15): the estimates of overall relative biomass from the spatial model

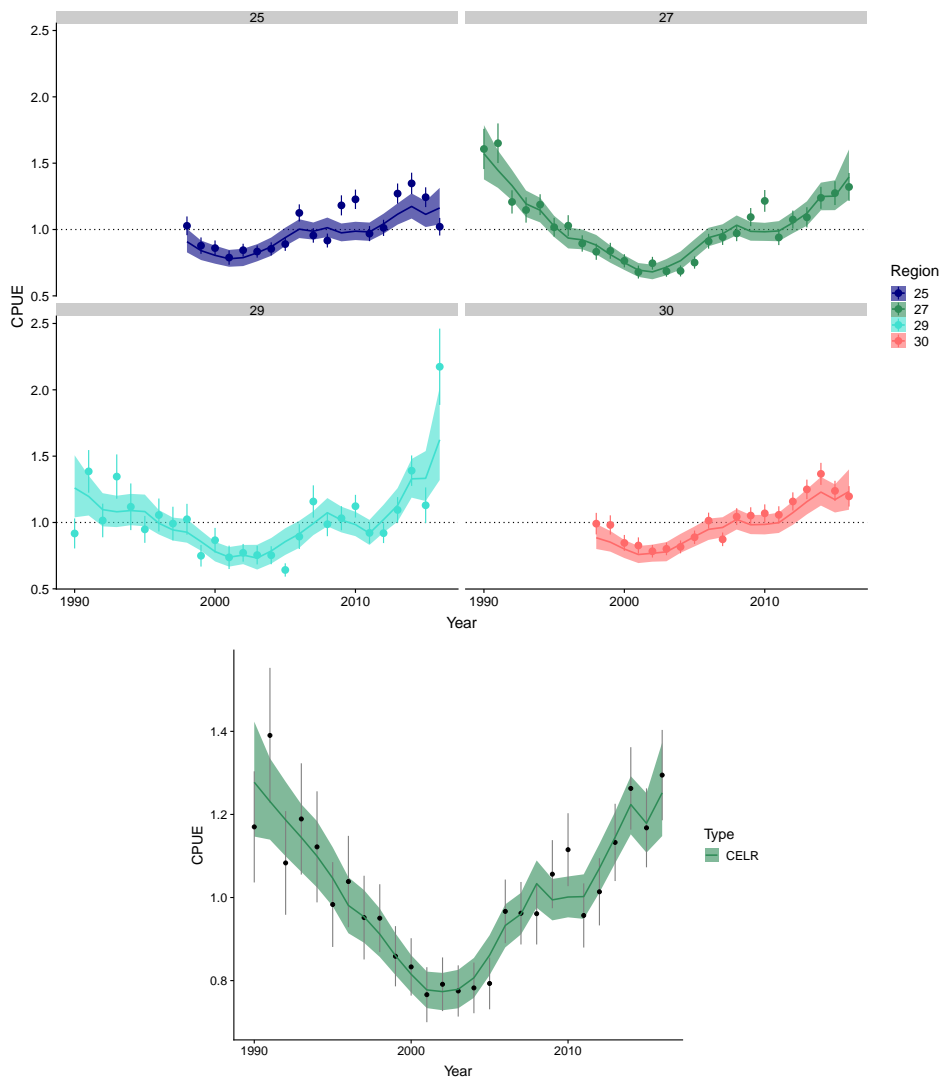


**Figure 8: Comparison of catch-per-unit-effort (CPUE) indices (black points and vertical observation error bars) and model fits (posterior median and 95% confidence interval as coloured ribbons) for regions in the spatial model (top four panels) and the single-area model (bottom panel; CELR, Catch Effort Landing Return) for pāua management area PAU 5B.**

were considerably higher than estimates from the single-area assessment (Figures 14 to 16). The reason for this discrepancy is most likely the difference in the catch history between the spatial and non-spatial models and its influence on the overall model dynamics. For the single-area model, reductions in catch in the early 2000s can be linked to a biomass rebuild at the same time across the region. In the spatial model, these synchronous increases in biomass cannot be linked to catch reductions since these reductions largely affected area 26 (the Catlins region), whereas catch in other areas remained stable. As a result, the model indicated higher overall biomass by forcing slower growth (and less available biomass to the fishery; Figure 17) and a larger overall stock size (Figure C-13).

In view of the relatively flat CPUE trend over the longer time series, fits to CPUE were not compromised by this adjustment between the single and multi-area models (Figure 18). Nevertheless, fits to CSLF trends were notably worse for the spatial model (Figures C-14, C-15) in contrast to the model for PAU 5B (Figures C-10, C-11). In addition, the recruitment patterns between the spatial and single-area models were markedly different for PAU 5D: the single-area model showed a regular “pulsed” recruitment pattern, whereas the spatial model created a large single year-class in the early 2000s to explain the increase in CPUE during that time (Figure 19).

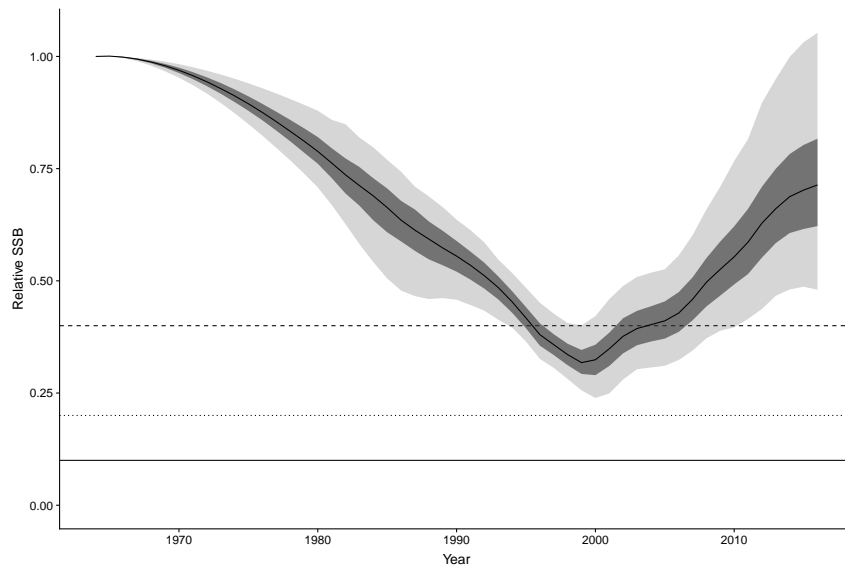


**Figure 9:** Relative biomass trend for pāua management area PAU 5B summed across all regions in the spatial model (i.e., by summing the biomass across regions and then calculating the relative spawning stock biomass, SSB).

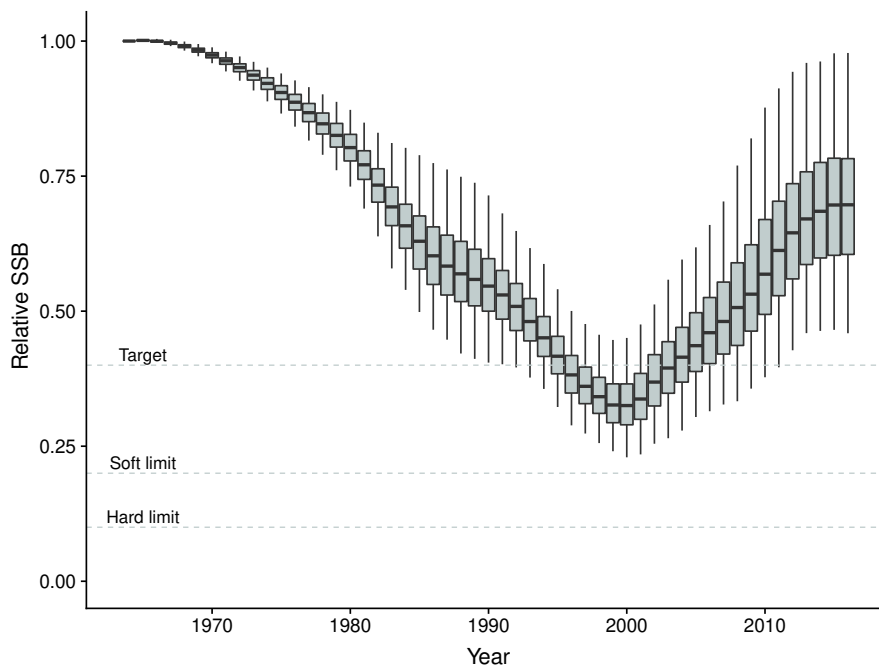


**Figure 10:** Relative spawning stock biomass (SSB) trend for pāua management area PAU 5B for the single-area assessment.

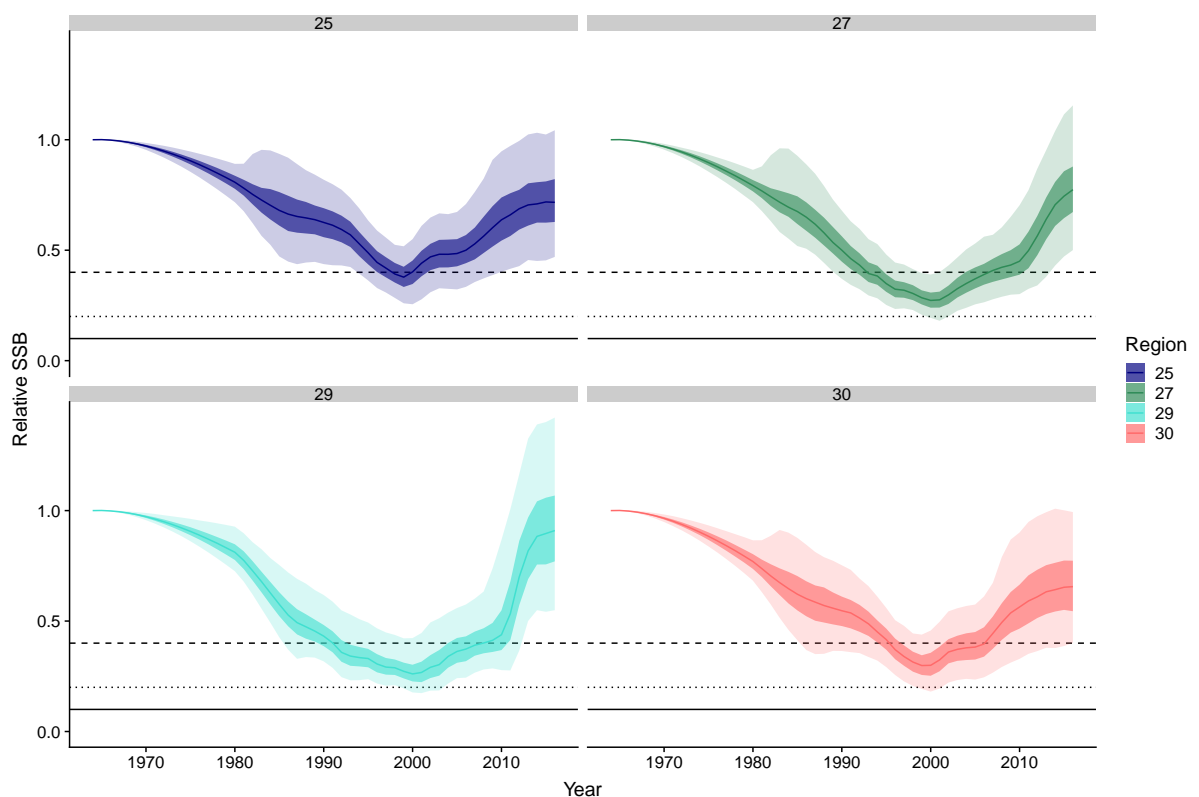


**Figure 11: Comparison of relative spawning stock biomass (SSB) trends for pāua management area PAU 5B for four regions in the spatial model.**

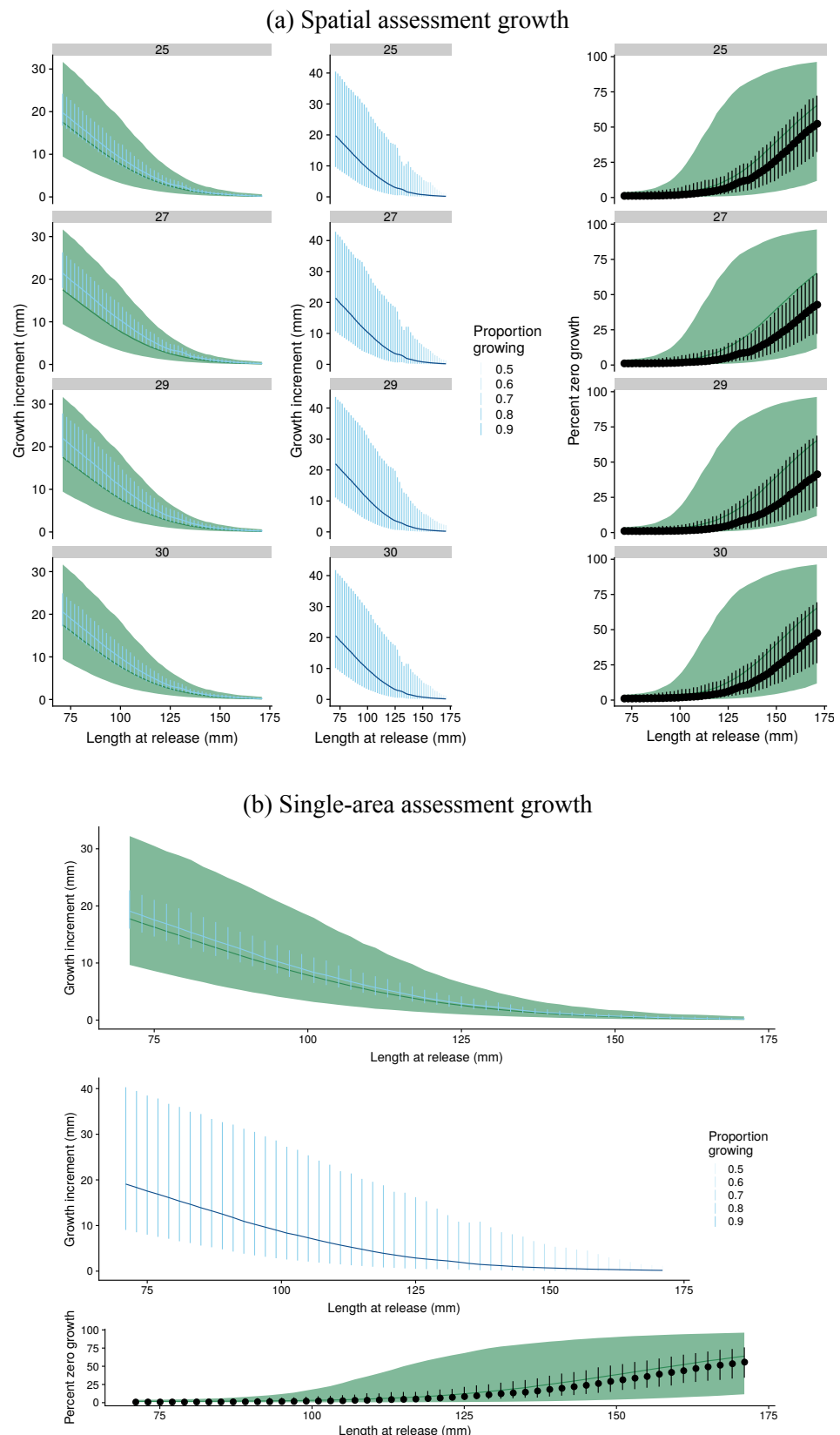


**Figure 12: Pāua population growth for four regions (25, 27, 29, 30) in the spatial model for PAU 5B (a) and the single area model (b). Shown in (a) are for each each model/region the posterior population mean growth (light blue line) and standard deviation (light blue vertical lines), the prior for population mean growth, and the prior 95% confidence interval (left); the population mean growth (blue line) and population standard deviation (light blue vertical lines) (middle); and the proportion of pāua stock not growing at each length (right). Arrangement in (b) of these graphs is top to bottom.**

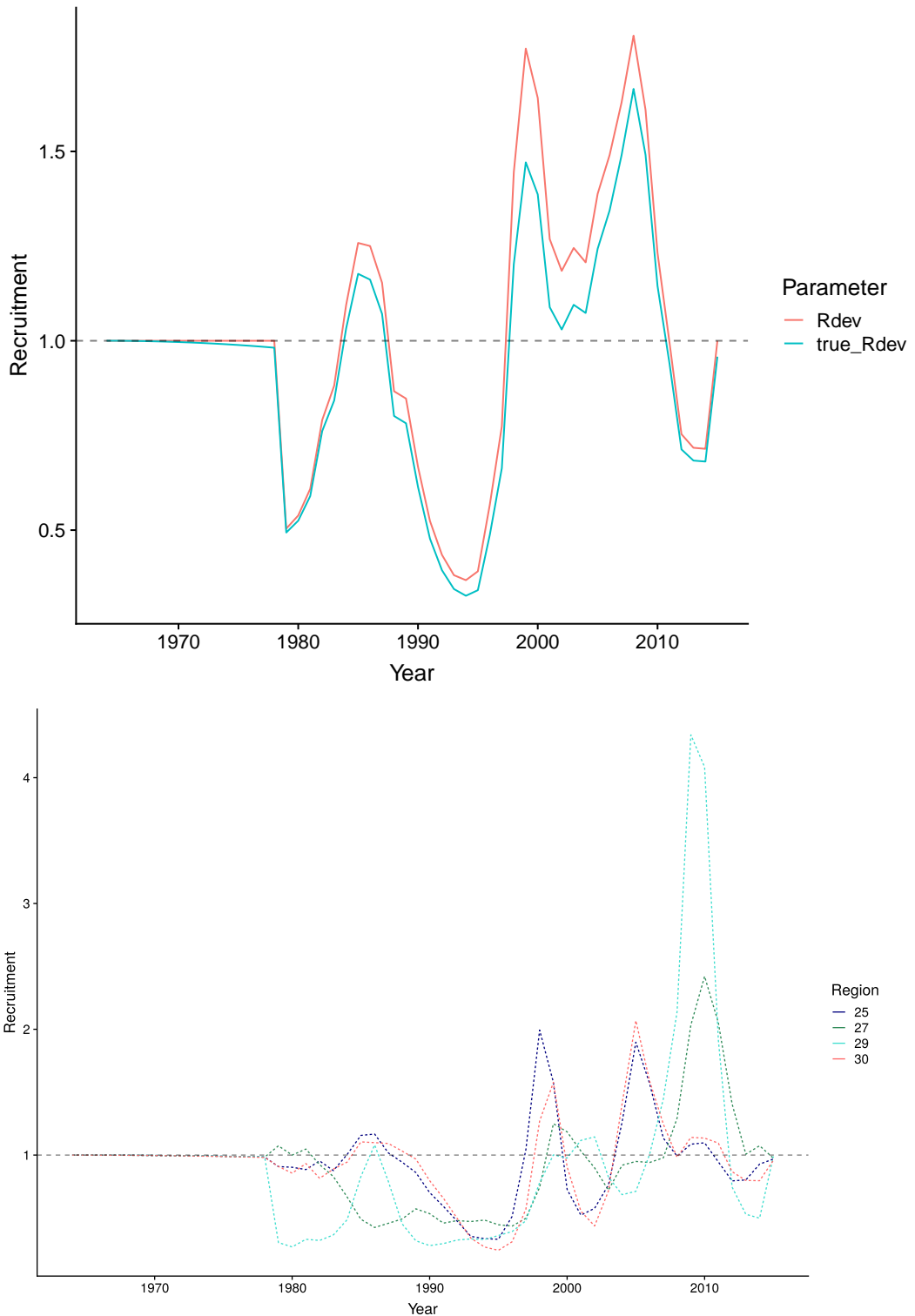


**Figure 13: Estimated recruitment deviations from the single-area model, and for four areas from the spatial assessment model for pāua management area PAU 5B.**

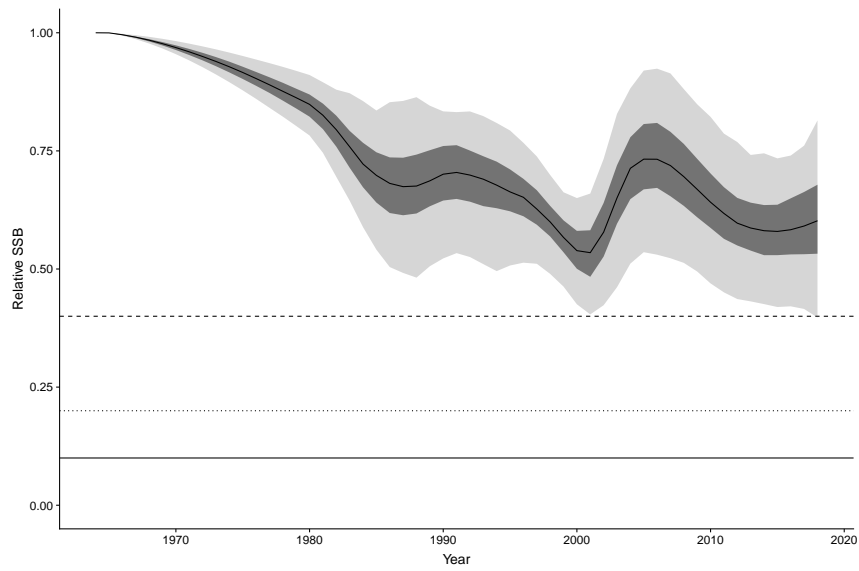


**Figure 14:** Relative biomass trend for pāua management area PAU 5D summed across all regions in the spatial model (i.e., by summing the biomass across regions and then calculating the relative spawning stock biomass, SSB).

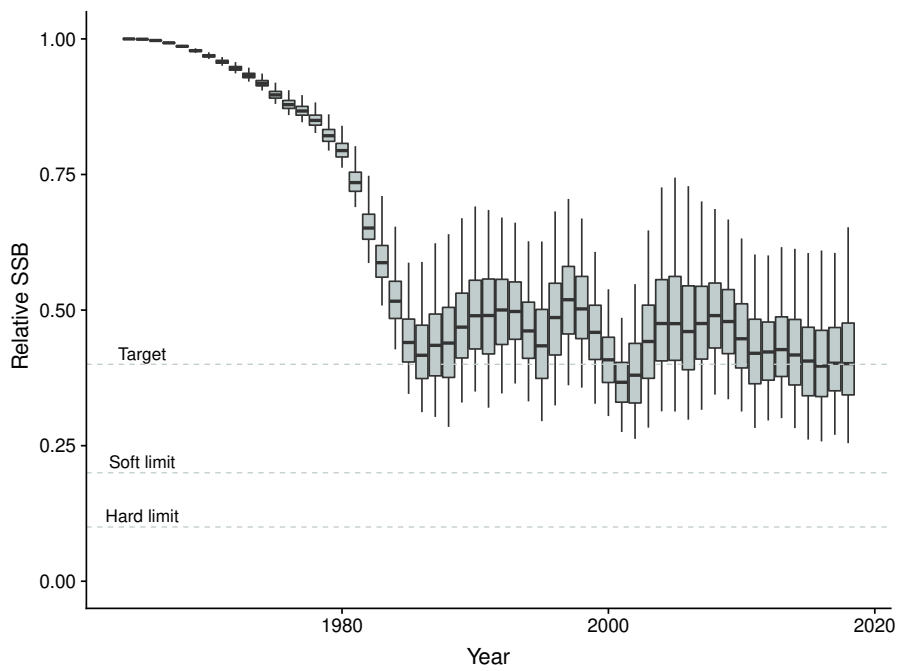


**Figure 15:** Relative spawning stock biomass (SSB) trend for pāua management area PAU 5D for the single-area assessment.

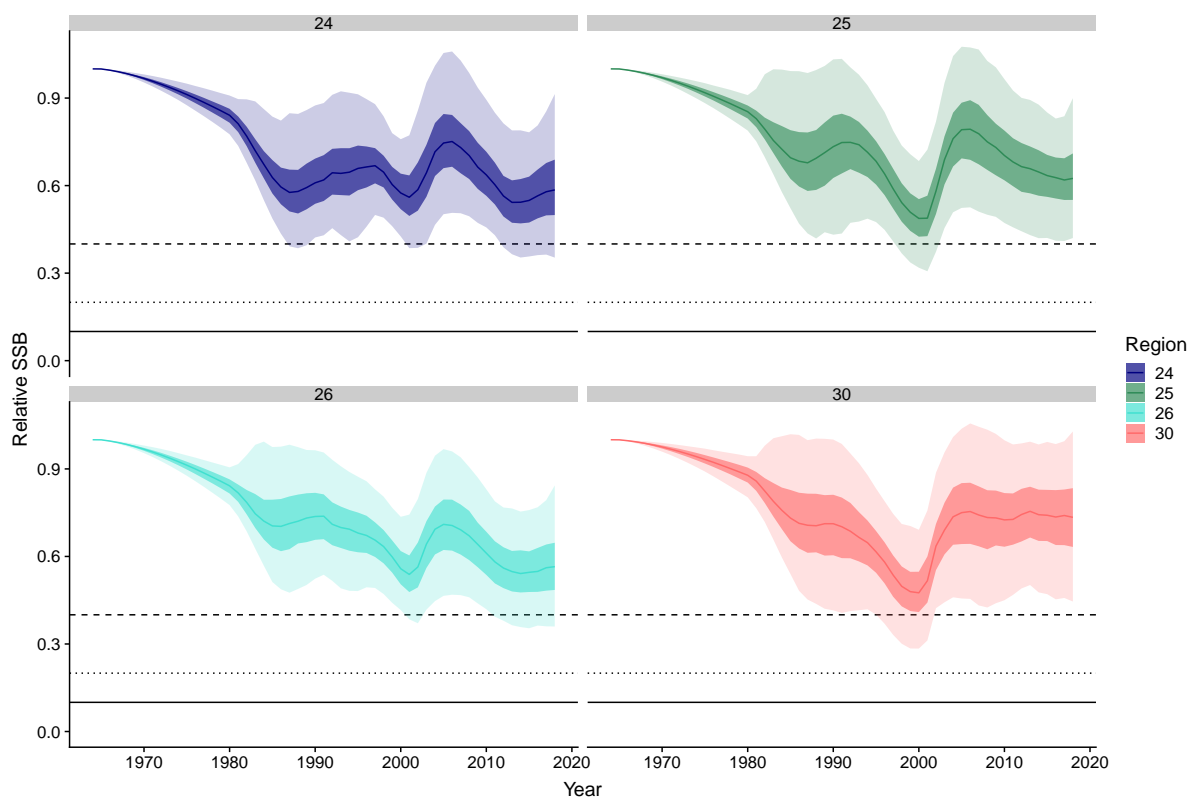


**Figure 16: Comparison of relative spawning stock biomass (SSB) trends for pāua management area PAU 5D for four regions in the spatial model.**

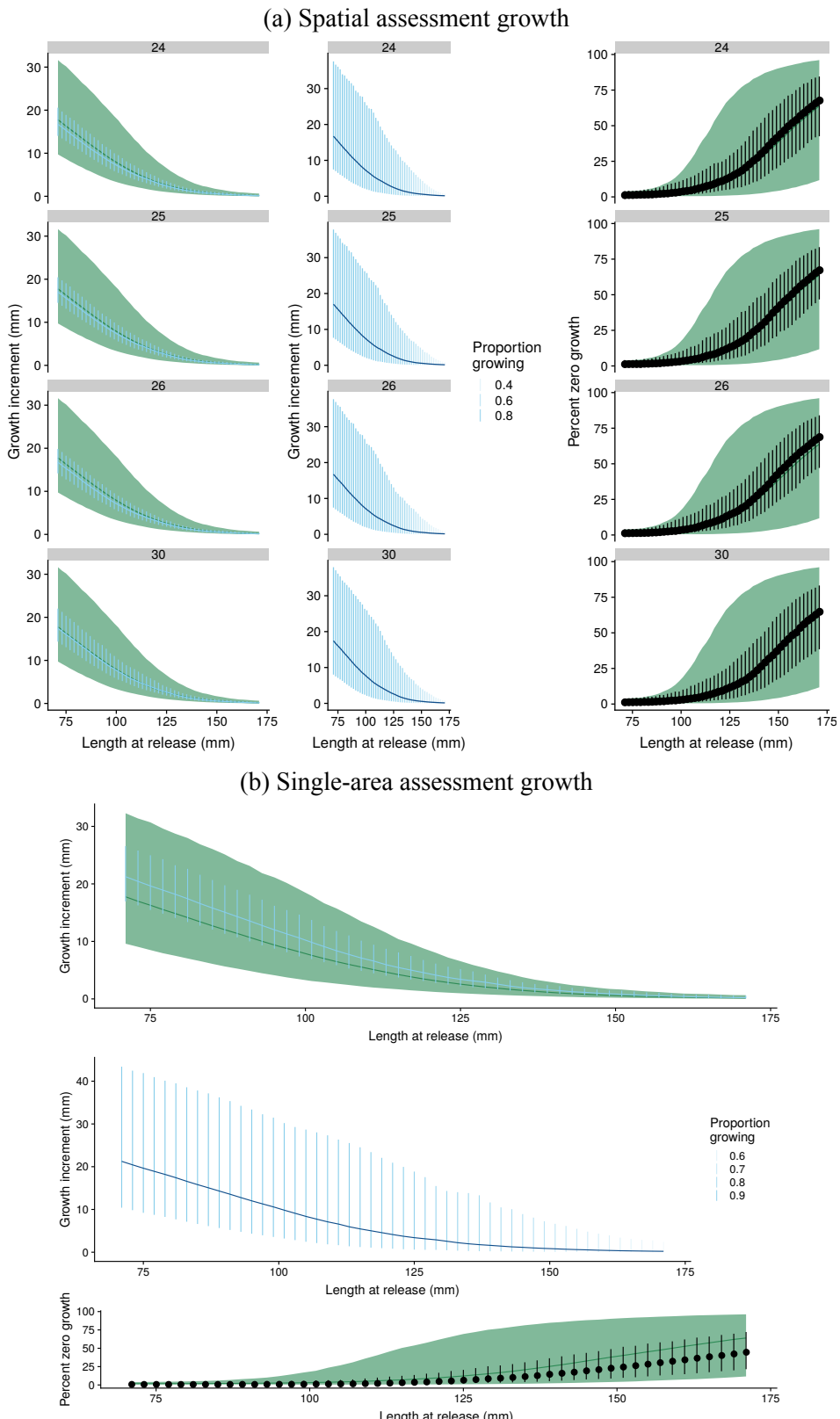


**Figure 17: Pāua population growth for four regions (24, 25, 26, 30) in the spatial model for PAU 5D (a) and the single-area model (b). Shown in (a) are for each each model/region the posterior population mean growth (light blue line) and standard deviation (light blue vertical lines), the prior for population mean growth, and the prior 95% confidence interval (left); the population mean growth (blue line) and population standard deviation (light blue vertical lines) (middle); and the proportion of pāua stock not growing at each length (right). Arrangement in (b) of these graphs is top to bottom.**

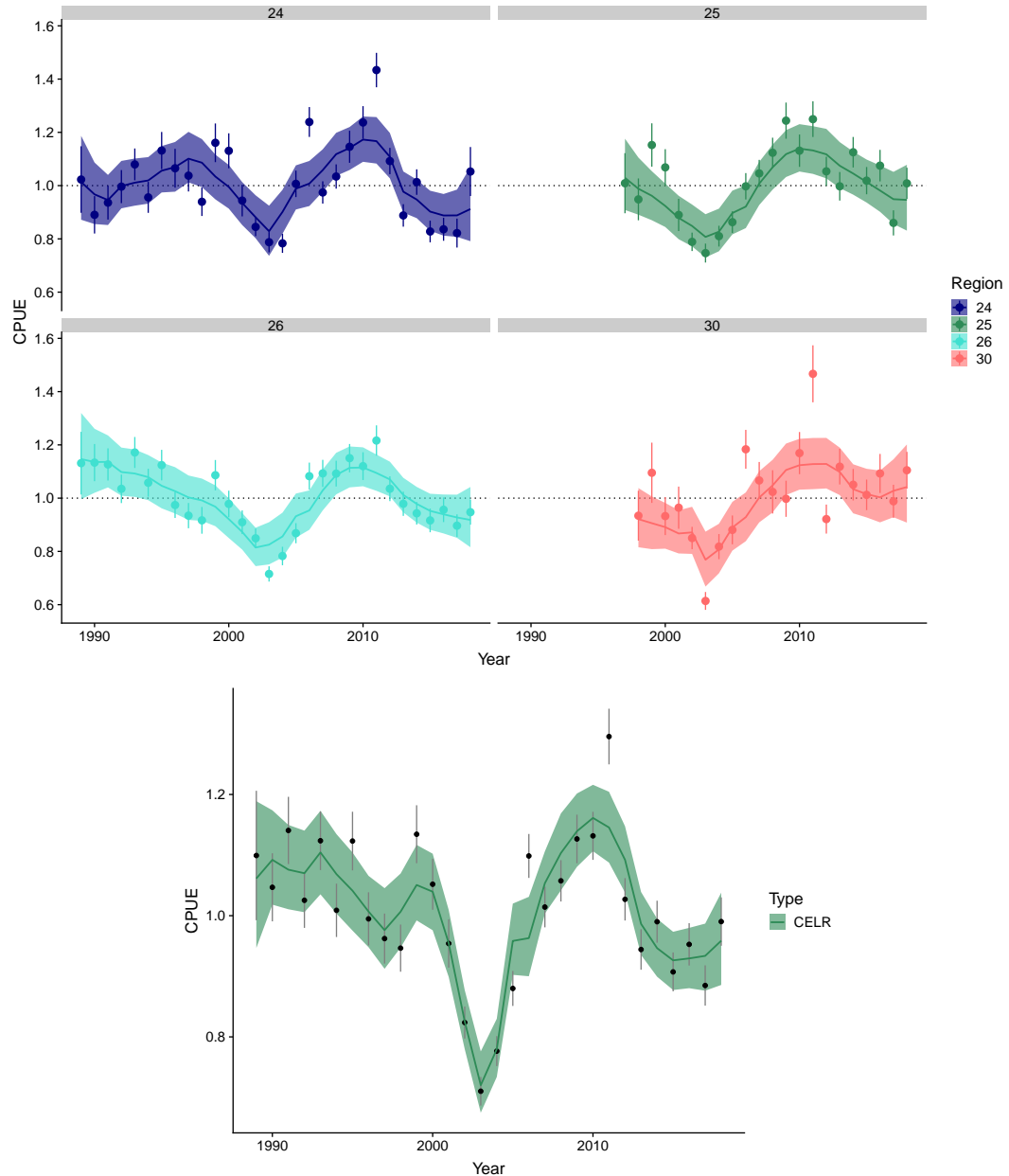


**Figure 18: Comparison of catch-per-unit-effort (CPUE) indices (points and vertical observation error-bars) and model fits (posterior median and 95% confidence interval as coloured ribbons) for regions in the spatial model (top four panels) and the single-area model (bottom panel; CELR, Catch Effort Landing Return) for pāua management area PAU 5D.**

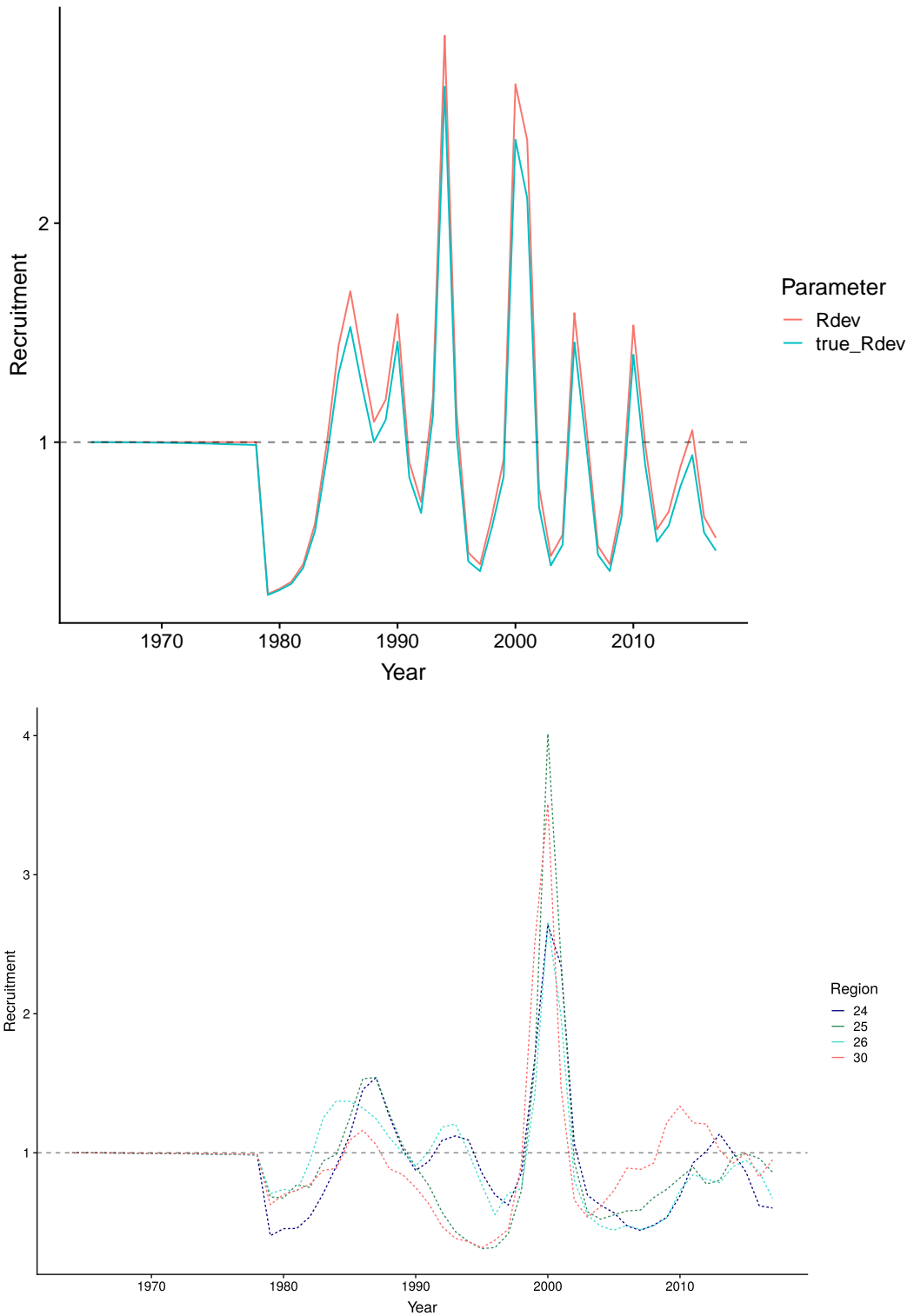


**Figure 19: Estimated recruitment deviations from the single-area model, and for four areas from the spatial assessment model for pāua management area PAU 5D.**

#### **4. DISCUSSION**

This project represents a first attempt at developing and fitting multi-area stock assessment models for pāua stocks, which are known to show considerable spatial variability in growth and other demographic parameters (McShane & Naylor 1995, Prince 2005, Naylor et al. 2006).

Differences between the spatial model and the single-area model for pāua management area PAU 5D highlight the importance of spatial dynamics in both catch (CPUE) and demographic parameters on inferred population dynamics, and the effects of fishing (Punt 2003, Cope & Punt 2011, Punt 2019b). In PAU 5D, it is difficult to reconcile the spatial variability in catch trends with a large effect of fishing. The structure of the single-area model cannot account for spatial differences in catch and, therefore, attributes changes in CPUE and available biomass to fishing. In contrast, the spatial model attempts to determine an alternative explanation for the CPUE trends, because catch by itself cannot explain increases in biomass in the early 2000s; the model, therefore, adjusts the overall biomass and growth. Whether the adjustment of biomass, and of the effect of fishing, between models represents a more realistic scenario is uncertain: the spatial model also estimated smaller than average growth for pāua in PAU 5D (compared with considerably greater than average growth for PAU 5B), which may not be regarded as a reasonable estimate. Punt (2003) found that a simplified spatial length-based assessment was strongly biased for initial biomass when early CPUE was not available to adjust early biomass trends. Similarly, Cope & Punt (2011) found that a spatial model did not necessarily improve estimates across a range of scenarios, but found that accounting for spatial catch histories generally improved assessment performance when the spatial variation matched that of effective management. It is, therefore, difficult to determine whether the spatial model for PAU 5D removes or accentuates bias relative to the single area model for this QMA.

Regardless of whether the spatial model provides a realistic representation of biomass, it shows that past assumptions of fast growth across the area, coupled with a biomass that is vulnerable to the levels of past extraction, are not compatible with the observed catch patterns and the associated relative biomass trends as inferred from CPUE. This finding stresses the importance of CPUE and catch history in determining assessment outcomes (Punt 2003, Cope & Punt 2011), and suggests renewed focus on early catch time series, and revisiting of the suitability of Fisheries Statistics Unit CPUE data. The latter had been discarded in recent assessments given the poor coverage of fishery catch in the corresponding years (1983–1988). Nevertheless, if the absence of early CPUE biases assessment outcomes, then having under-representative data may be preferable to the lack of data for that period.

Spatial assessment and management tools are reliant on spatially resolved data, and current efforts to collect growth data across a more representative area of all QMAs will contribute to resolving spatially varying growth patterns. Growth firmly dictates inferences about stock status from the model (Neubauer & Tremblay-Boyer 2019b), and obtaining a better understanding of spatial variations in growth appears the most promising way to improve the robustness of pāua assessments (see also Plagányi & Butterworth 2010). Nevertheless, the current method of obtaining samples from distinct points in space only measures growth at a single site; it may be difficult to construct a representative assessment of growth across smaller areas from this limited sampling, even with a large number of sites sampled. Alternative programme structures that tag pāua over larger areas (at the expense of recapture rates) could be considered to broaden the spatial extent of the data and its representation for growth across the different QMAs and smaller areas. Another valuable approach would be to gain improved mechanistic understanding of pāua growth so that growth can be predicted in space, based on observed growth data and the identification of factors determining it (i.e., temperature, coastline exposure, primary production, pāua density).

A greater understanding of spatial variability in demography, combined with the real-time electronic reporting of CPUE that will be available from 2019, will enable the development of models that incorporate greater spatial complexity; the latter can then be used to assess and test management at smaller spatial scales (Berger et al. 2017). Examples of these smaller management units include the spatial scale of statistical area and CPUE limits, and also strategies to spread effort to avoid local depletion. Across larger spatial scales, the spatial model can provide a tool to assess areas like PAU 5A as a single area, instead of the current practice of splitting the area into two assessments. Similarly, for other areas that

span fishing grounds with contrasting fishing histories, such as PAU 7 (east coast of Marlborough south of Cape Campbell; Cook Strait and D'Urville Island), these areas could be assessed in a spatial assessment to test the impact of Total Allowable Commercial Catch adjustments in view of uneven spatial effort distributions (e.g., no fishing in the closed area on the eastern Marlborough coast since the 2016 Kaikōura earthquake).

In summary, the spatial model could fulfill three roles:

1. Testing the impact of assumptions of spatial homogeneity in catch and demographic parameters on assessment outcomes.
2. Assessing quota management areas with considerably different fisheries to allow evaluation of QMA-wide management measures and potential impact on smaller regions.
3. Uncovering key uncertainties and guiding research priorities for pāua stocks.

## 5. ACKNOWLEDGMENTS

Many thanks to the members of the Shellfish Working Group for stimulating discussion and ideas that led to the development of this model.

This work was funded by Ministry for Primary Industries project PAU2017-03.

## 6. REFERENCES

- Abraham, E.R. (2012). Pāua catch per unit effort from logger data. Final Research Report for Ministry for Primary Industries project PAU2010-03 (Unpublished report held by Ministry for Primary Industries, Wellington). Retrieved from [http://fs.fish.govt.nz/Doc/23163/2013-03\\_2621\\_PAU2010-03\\_MS3\\_fighting-bay%20final%20FRR.pdf.ashx](http://fs.fish.govt.nz/Doc/23163/2013-03_2621_PAU2010-03_MS3_fighting-bay%20final%20FRR.pdf.ashx).
- Berger, A.M.; Goethel, D.R.; Lynch, P.D.; Quinn, T.; Mormede, S.; McKenzie, J.; Dunn, A. (2017). Space oddity: The mission for spatial integration. *Canadian Journal of Fisheries and Aquatic Sciences* 74 (11): 1698–1716.
- Breen, P.A.; Kim, S.W.; Andrew, N.L. (2003). A length-based Bayesian stock assessment model for the New Zealand abalone *Haliotis iris*. *Marine and Freshwater Research* 54 (5): 619–634.
- Cadrin, S.X.; Goethel, D.R.; Morse, M.R.; Fay, G.; Kerr, L.A. (2019). “So, where do you come from?” The impact of assumed spatial population structure on estimates of recruitment. *Fisheries Research* 217: 156–168.
- Cope, J.M.; Punt, A.E. (2011). Reconciling stock assessment and management scales under conditions of spatially varying catch histories. *Fisheries Research* 107 (1): 22–38.
- Fu, D. (2014). The 2013 stock assessment of paua (*Haliotis iris*) for PAU 5B. *New Zealand Fisheries Assessment Report 2014/45*. 51 p.
- Gelman, A.; Hill, J. (2006). Data analysis using regression and multilevel/hierarchical models. 648 p. Cambridge University Press, Cambridge.
- Goethel, D.R.; Quinn, T.J.; Cadrin, S.X. (2011). Incorporating spatial structure in stock assessment: Movement modeling in marine fish population dynamics. *Reviews in Fisheries Science* 19 (2): 119–136.
- Marsh, C.; Fu, D. (2017). The 2016 stock assessment of paua (*Haliotis iris*) for PAU 5D. *New Zealand Fisheries Assessment Report 2017/33*. 48 p.
- McShane, P.; Naylor, J.R. (1995). Small-scale spatial variation in growth, size at maturity, and yield-and egg-per-recruit relations in the New Zealand abalone *Haliotis iris*. *New Zealand Journal of Marine and Freshwater Research* 29 (4): 603–612.
- McShane, P.E. (1998). Assessing stocks of abalone (*Haliotis* spp.): Methods and constraints. *Canadian Special Publication of Fisheries and Aquatic Sciences*: 41–48.
- Naylor, J.; Andrew, N.; Kim, S. (2006). Demographic variation in the New Zealand abalone *Haliotis iris*. *Marine and Freshwater Research* 57 (2): 215–224.

- Neubauer, P. (2019). Development and evaluation of management procedures in pāua quota management areas 5A, 5B and 5D. *New Zealand Fisheries Assessment Report 2019/37*. 63 p.
- Neubauer, P.; Tremblay-Boyer, L. (2019a). Input data for the 2018 stock assessment of pāua (*Haliotis iris*) for PAU 5D. *New Zealand Fisheries Assessment Report 2019/38*. 40 p.
- Neubauer, P.; Tremblay-Boyer, L. (2019b). The 2018 stock assessment of pāua (*Haliotis iris*) for PAU 5D. *New Zealand Fisheries Assessment Report 2019/39*.
- Neubauer, P.; Abraham, E.; Knox, C.; Richard, Y. (2014). Assessing the performance of pāua (*Haliotis iris*) fisheries using GPS logger data. Final Research Report for Ministry for Primary Industries project PAU2011-03 (Unpublished report held by Ministry for Primary Industries, Wellington).
- Plagányi, É.E.; Butterworth, D.S. (2010). A spatial- and age-structured assessment model to estimate the impact of illegal fishing and ecosystem change on the South African abalone *Haliotis midae* resource. *African Journal of Marine Science* 32 (2): 207–236.
- Prince, J. (2005). Combating the tyranny of scale for haliotids: Micro-management for microstocks. *Bulletin of Marine Science* 76 (2): 557–578.
- Punt, A.E. (2003). The performance of a size-structured stock assessment method in the face of spatial heterogeneity in growth. *Fisheries Research* 65 (1-3): 391–409.
- Punt, A.E. (2019a). Modelling recruitment in a spatial context: A review of current approaches, simulation evaluation of options, and suggestions for best practices. *Fisheries Research* 217: 140–155.
- Punt, A.E. (2019b). Spatial stock assessment methods: A viewpoint on current issues and assumptions. *Fisheries Research* 213: 132–143.
- Stan Development Team (2018). RStan: the R interface to Stan. R package version 2.17.3. Retrieved from <http://mc-stan.org/>.
- Thorson, J.T. (2014). Standardizing compositional data for stock assessment. *ICES Journal of Marine Science* 71 (5): 1117–1128. doi:10.1093/icesjms/fst224.
- Walters, C.J.; Martell, S.J.; Korman, J. (2006). A stochastic approach to stock reduction analysis. *Canadian Journal of Fisheries and Aquatic Sciences* 63 (1): 212–223.

## APPENDIX A: SUPPLEMENTARY FIGURES

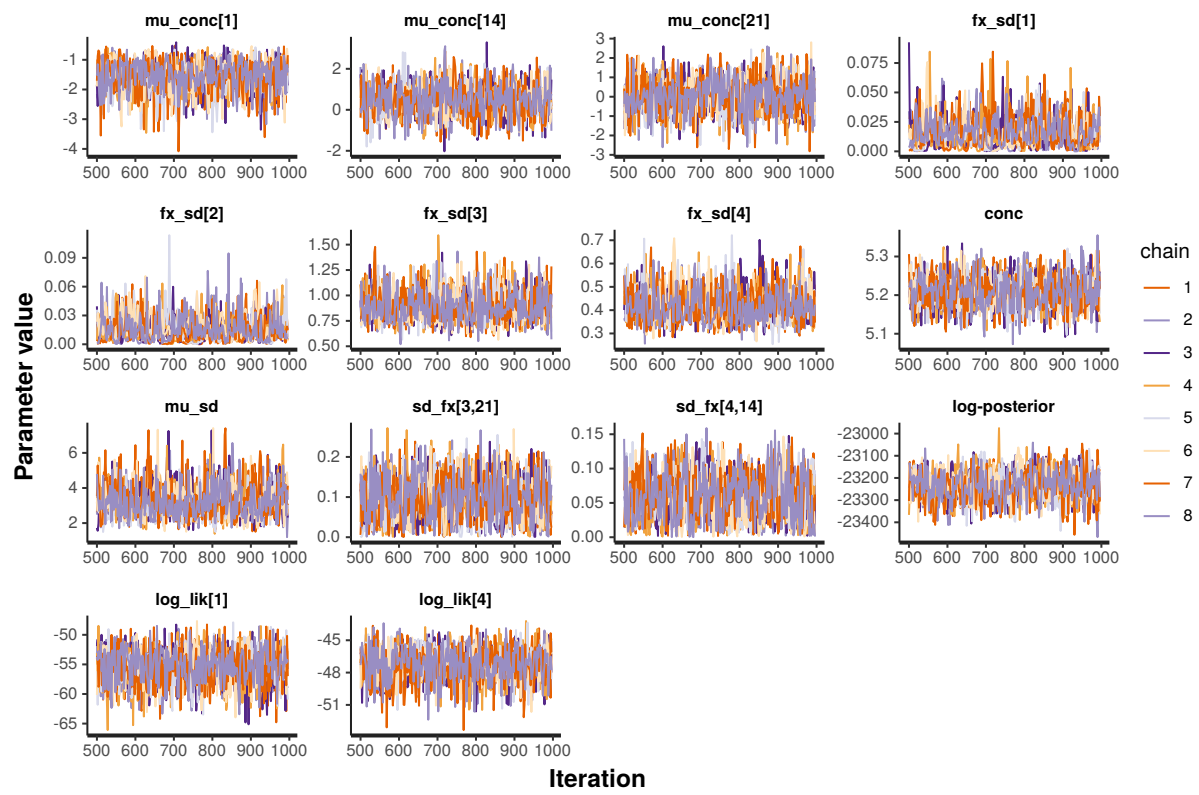


**Figure A-1: Markov chain Monte Carlo (MCMC) traces for selected parameters in the Dirichlet-Multinomial length composition standardisation model for pāua management area PAU 5B. (Results were almost identical for PAU 5D.)**

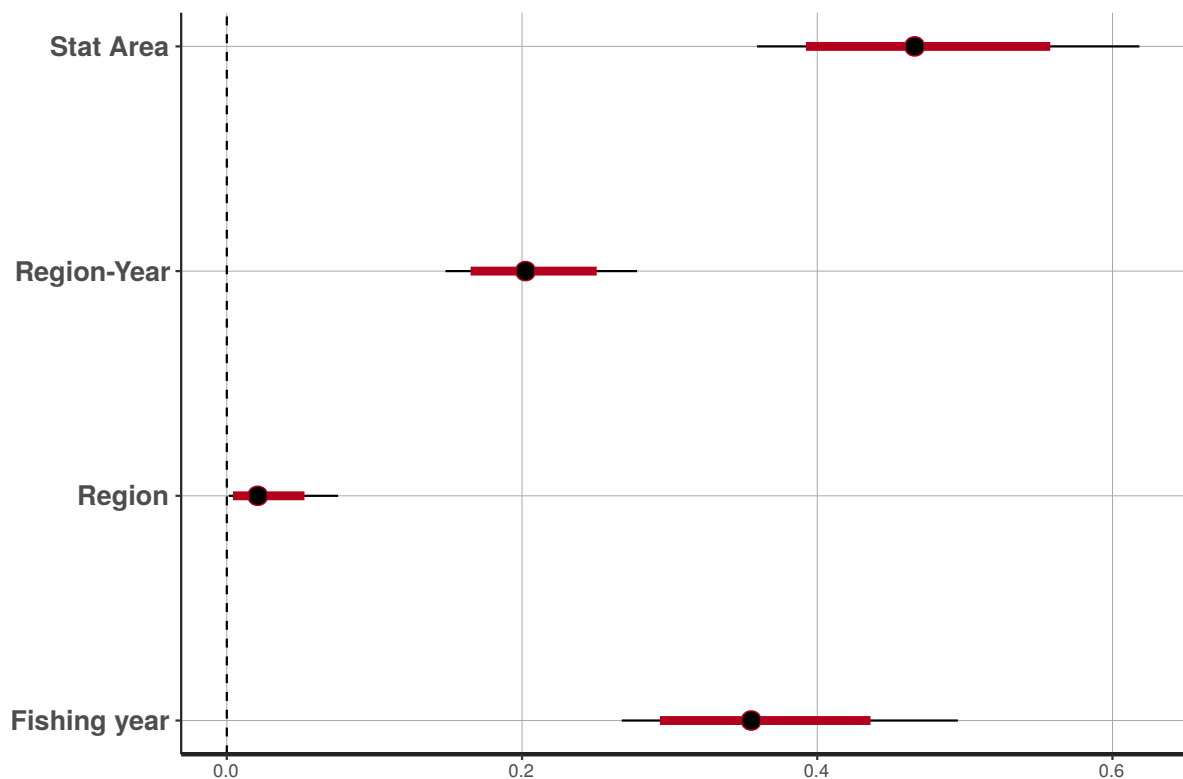


**Figure A-2:** Dirichlet-Multinomial posterior distributions for random effects variance parameters  $\sigma$  for pāua management area PAU 5D. (Results were almost identical for PAU 5B.).

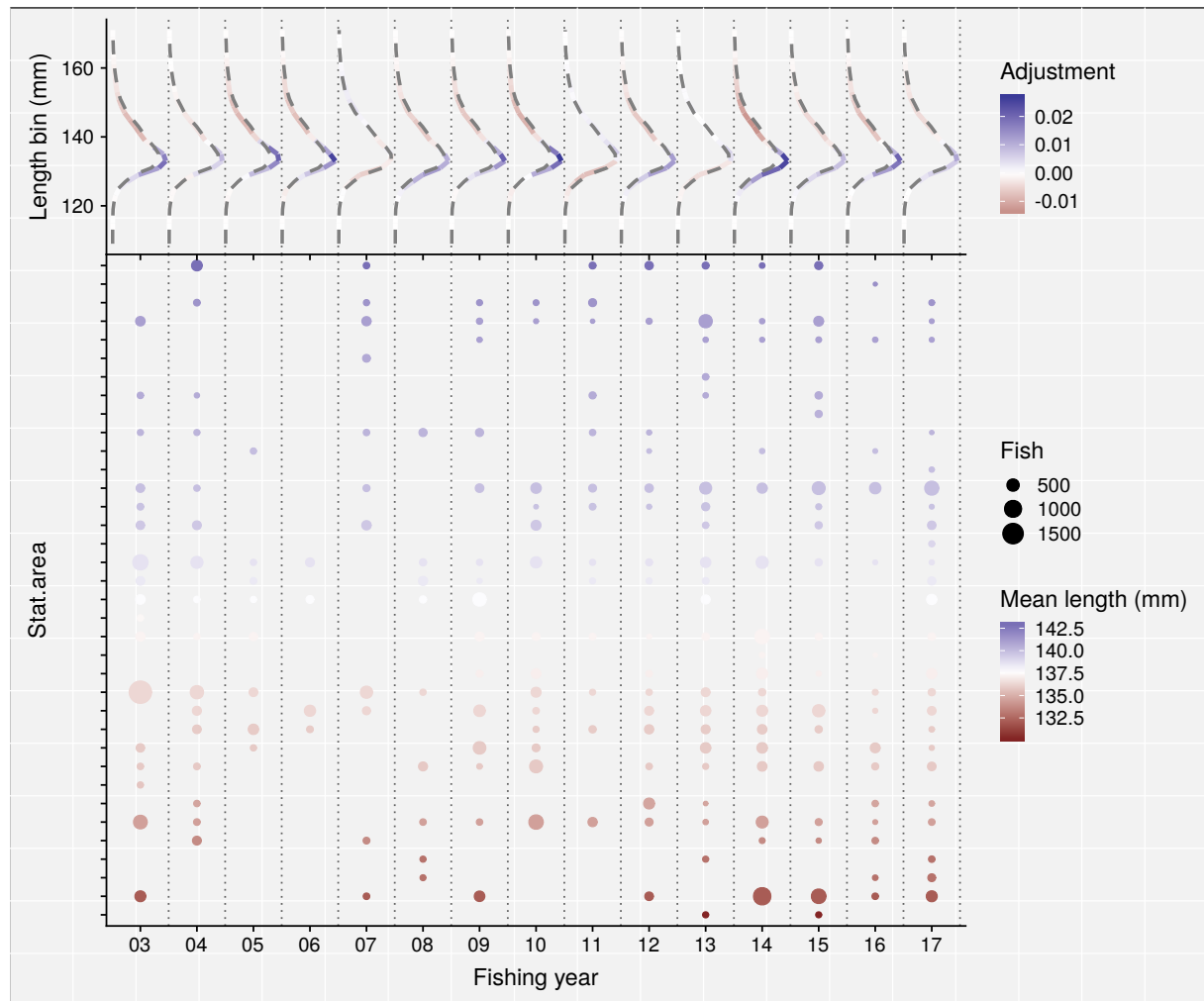


**Figure A-3: Statistical area effects plot for pāua management area PAU 5D.** Top panel displays the direction of deviation of the raw catch sampling length frequency data in each year and length bin (class) in relation to the fishing pattern (shown in the lower panel). Statistical areas in the lower panel are sorted by the observed mean length to allow comparisons of their influence on estimated deviations in the upper panel. (Results were nearly identical for PAU 5B.)

## APPENDIX B: PRIOR PREDICTIVE SIMULATIONS

The following section illustrates prior predictive simulations used to justify priors on  $R_0$  and  $\lambda$  for PAU 5B. (Results were nearly identical for PAU 5D.)

### B.1 Uniform priors

With near uniform priors on both  $R_0$  (Uniform(6, 30)) and  $\lambda$  (Dirichlet( $1/n_{regions}$ )), much of the probability mass of these priors falls outside of plausible outcome space for the assumed model: low  $R_0$  or any  $\lambda_r$  near 0 (for any of the regions) leads to a quick and complete depletion of available biomass in one or all regions (Figure B-4).

### B.2 Informed priors

With informed priors on  $R_0$  only (using the same prior as for the single-area assessments), much of the parameter space remains non-feasible, and few samples are retained when exploitation rates are restricted to a plausible space of  $<1$  and  $>0.01$ . From the retained sample for  $\lambda$ , it appears that the prior based on catch proportions provides a reasonable approximation to the retained prior  $\lambda$  values (Figure B-5).

With informed priors for both  $R_0$  and  $\lambda$ , the implied priors for stock status (Figure B-6) and maximum depletion (Figure B-7) for the stock are constrained to lie within plausible regions of the outcome space for the assumed model: while maximum depletion over the time series has a high probability of having been near the soft limit (20% of unfished spawning stock biomass), the mode of the prior on current depletion is situated at higher relative biomass levels given large reductions in catch in the early 2000s.

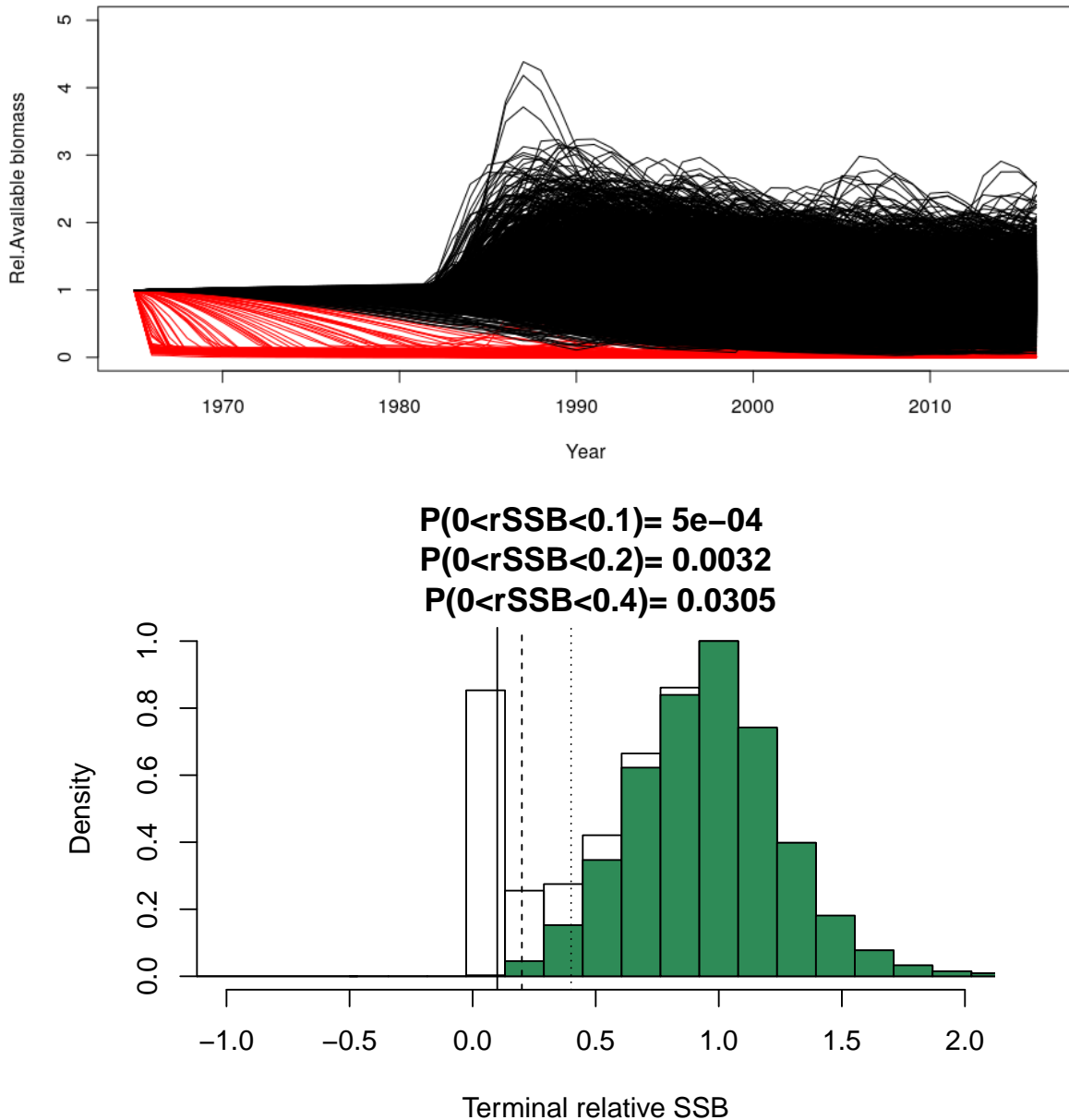


**Figure B-4: Population trajectories (top graph) for a single region (area 25) in PAU 5B for prior predictive simulations of stock dynamics with observed removals, using approximately uniform priors for both unfished recruitment  $R_0$  and the proportion of recruitment attributed to each region ( $\lambda$ ). Trajectories in red are discarded *a priori* because either i) exploitation rate in the focal region was  $>1$  in any one year, and/or ii) exploitation rate in any other region in the model was  $>1$  in any one year. The prior for stock status (relative spawning stock biomass, rSSB; bottom panel) after removing *a priori* discarded runs is centered around 1, with a low probability of being below any reference point.**

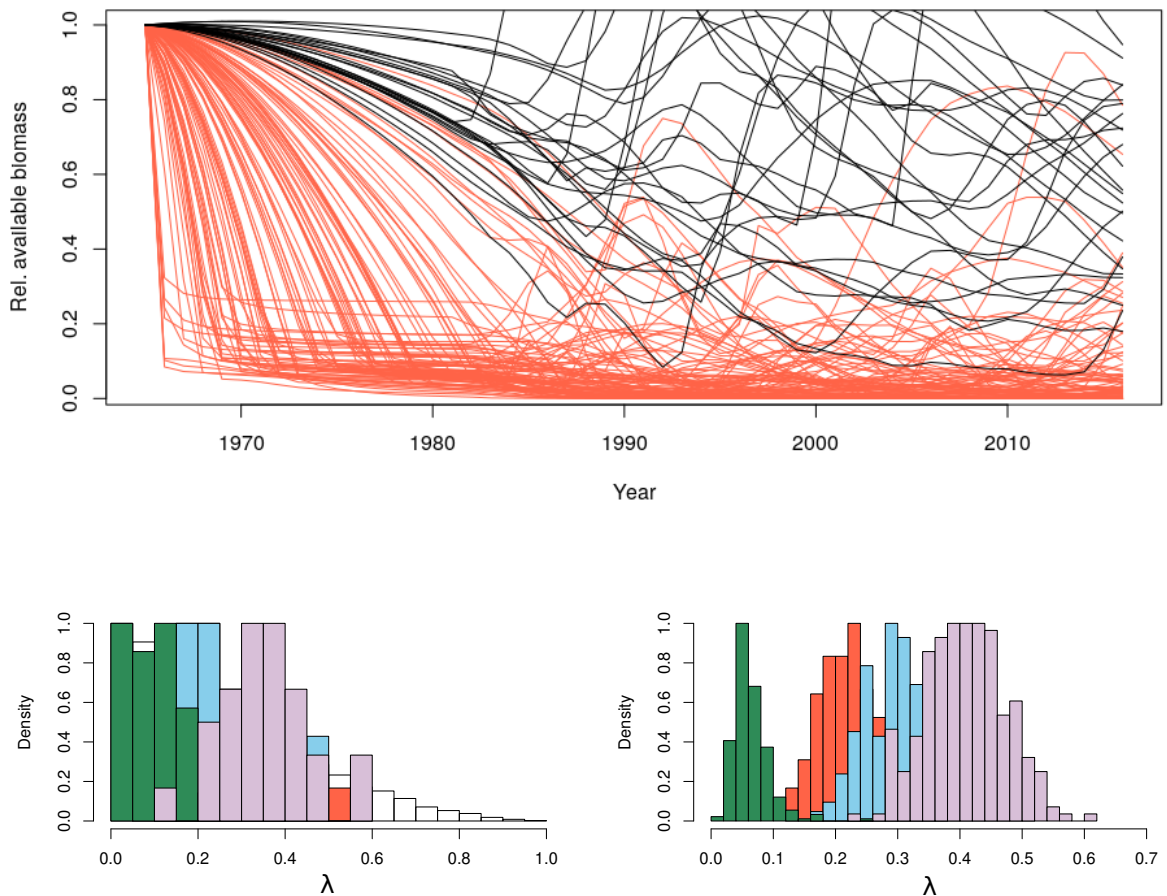


**Figure B-5: Population trajectories (top graph) for a single region (area 25) in PAU 5B for prior predictive simulations of stock dynamics with observed removals, using informed priors for both unfished recruitment  $R_0$  and the proportion of recruitment attributed to each region ( $\lambda$ ). Trajectories in red are discarded *a priori* because either i) exploitation rate in the focal region was  $>1$  in any one year, and/or ii) exploitation rate in any other region in the model was  $>1$  in any one year. Lower graphs show the values of  $\lambda$  that are retained with a uniform prior on  $\lambda$  and an informed prior on  $R_0$  (left graph), and the prior values of  $\lambda$  with an informed prior based on catch distributions among regions (indicated by different colours; green: area 29, red: area 27, blue: area 25, lavender: area 30 - right graph).**

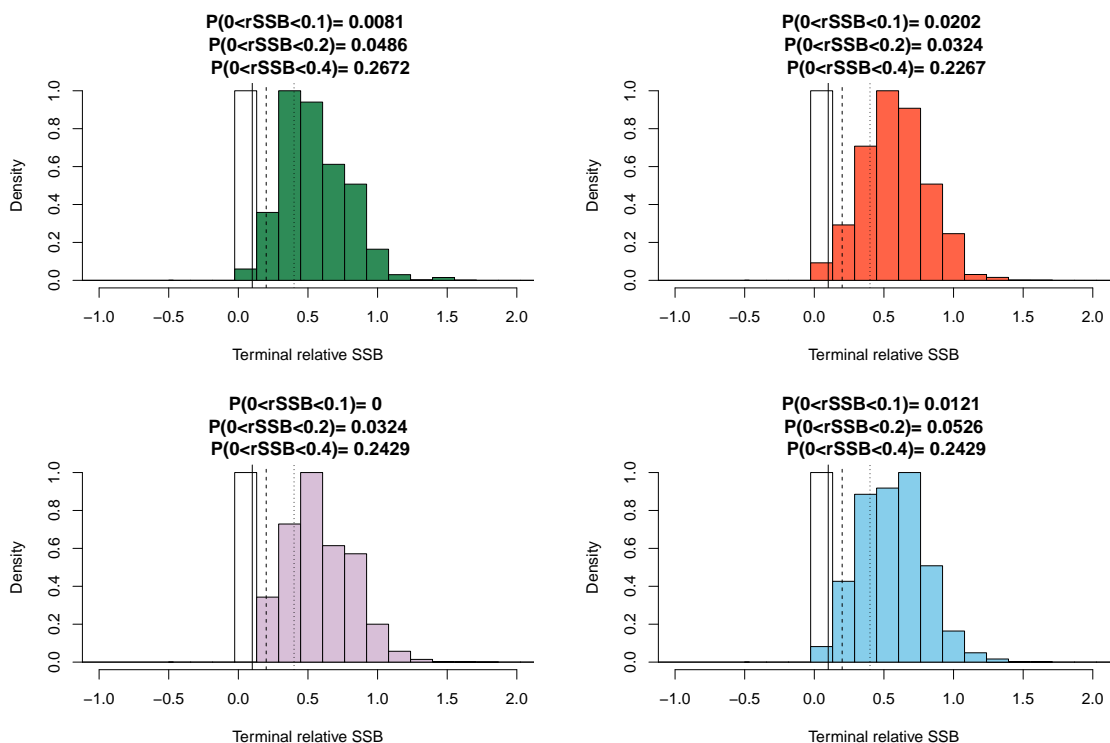


**Figure B-6:** Stock status of pāua (relative spawning stock biomass, rSSB) in 2017 for four regions in PAU 5B from prior predictive simulations of stock dynamics with observed removals, using informed priors for both unfished recruitment  $R_0$  and the proportion of recruitment ( $\lambda$ ) attributed to each region (indicated by different colours; green: area 29, red: area 27, blue: area 25, lavender: area 30).

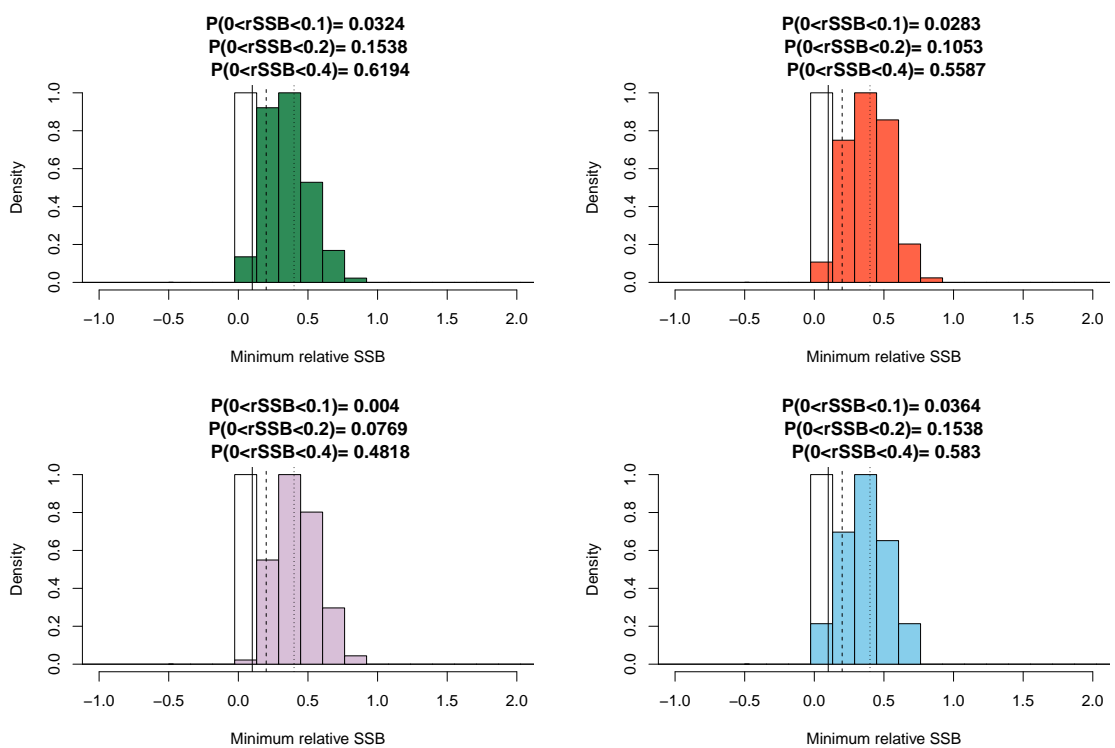


**Figure B-7: Maximum depletion over simulated population trajectories of pāua for four regions in PAU 5B from prior predictive simulations of stock dynamics (relative spawning stock biomass, rSSB) with observed removals, using informed priors for both unfished recruitment  $R_0$  and the proportion of recruitment ( $\lambda$ ) attributed to each region (indicated by different colours; green: area 29, red: area 27, blue: area 25, lavender: area 30).**

## APPENDIX C: MODEL COMPARISON

### C.1 PAU 5B

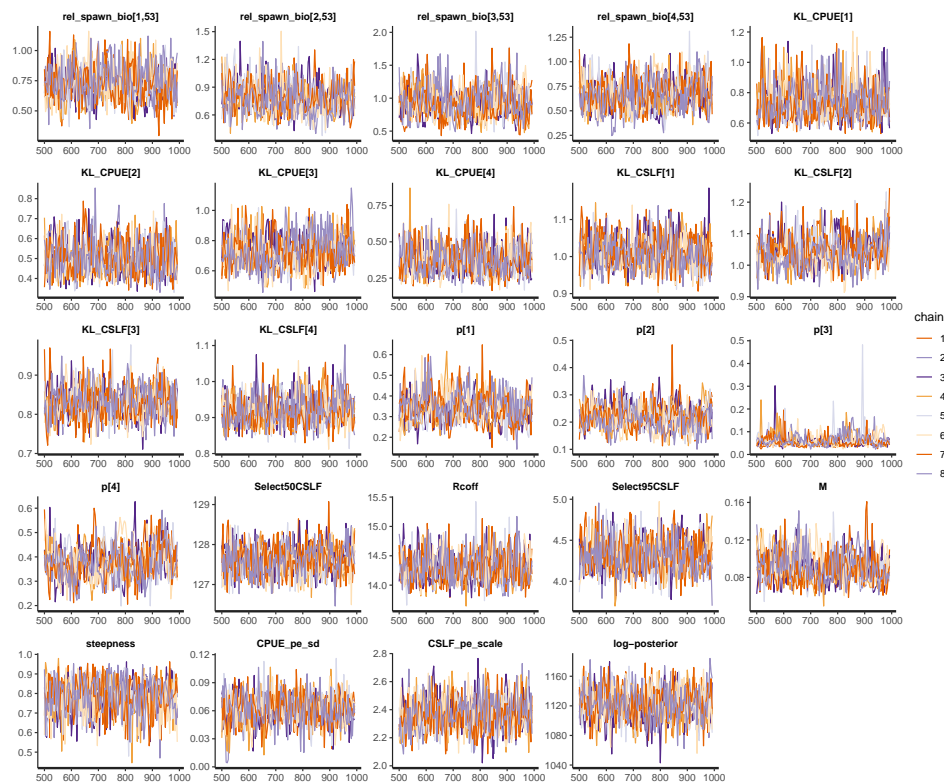


**Figure C-8: Markov chain Monte Carlo (MCMC) trace plots for key model parameters of the spatial stock assessment model for pāua in quota management area PAU 5B (blue); priors are shown as red line where applicable.**

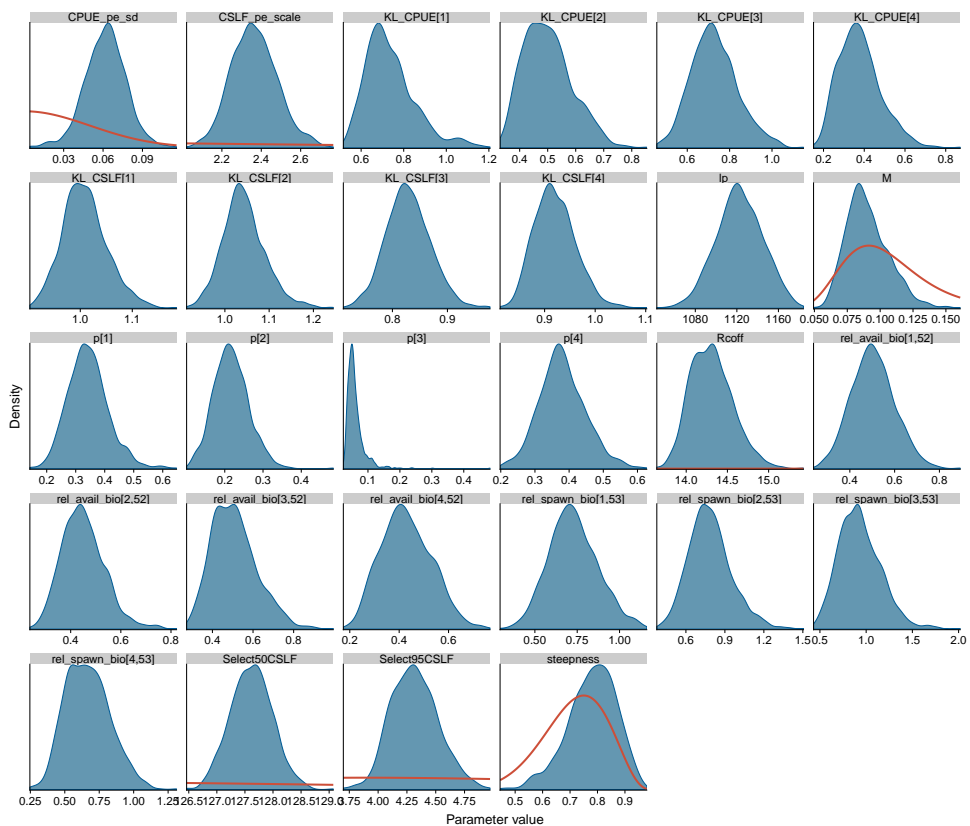


**Figure C-9: Marginal posterior densities for key model parameters of the spatial stock assessment model for pāua in quota management area PAU 5B (blue); priors are shown as red line where applicable.**

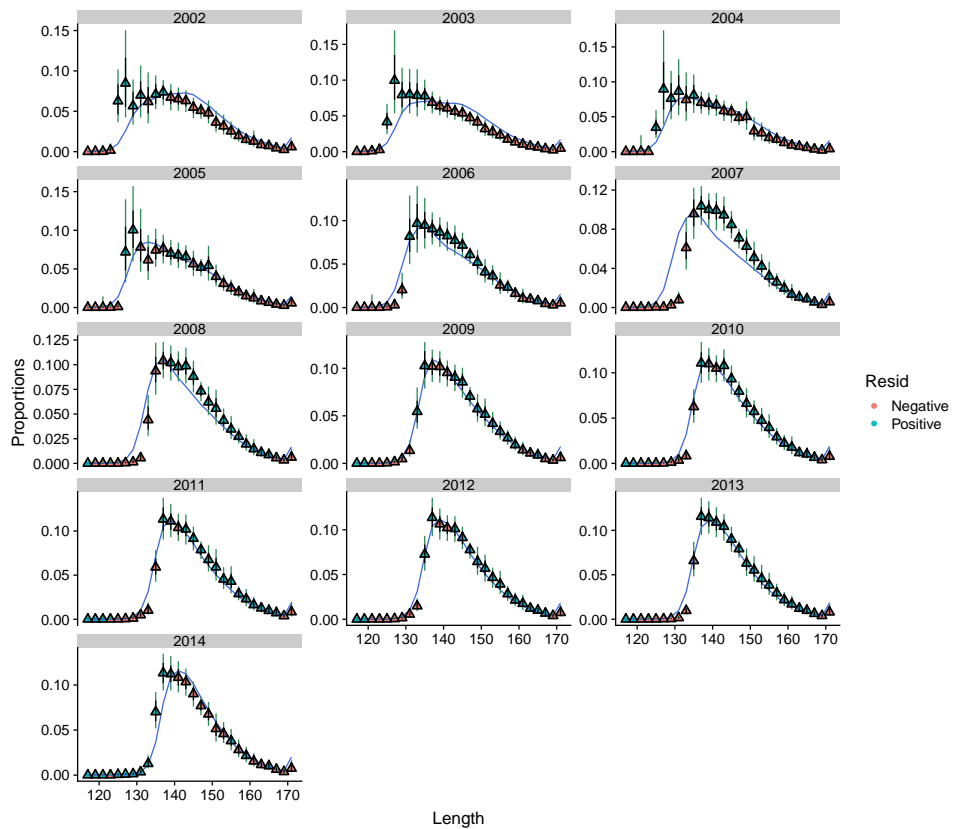


**Figure C-10: Comparison of posterior mean predicted catch sampling length frequency (CSLF) with estimated CSLF proportions and observation error for the single area stock assessment model for pāua in quota management area PAU 5B. Length classes with positive residuals in blue, with negative residuals in red.**

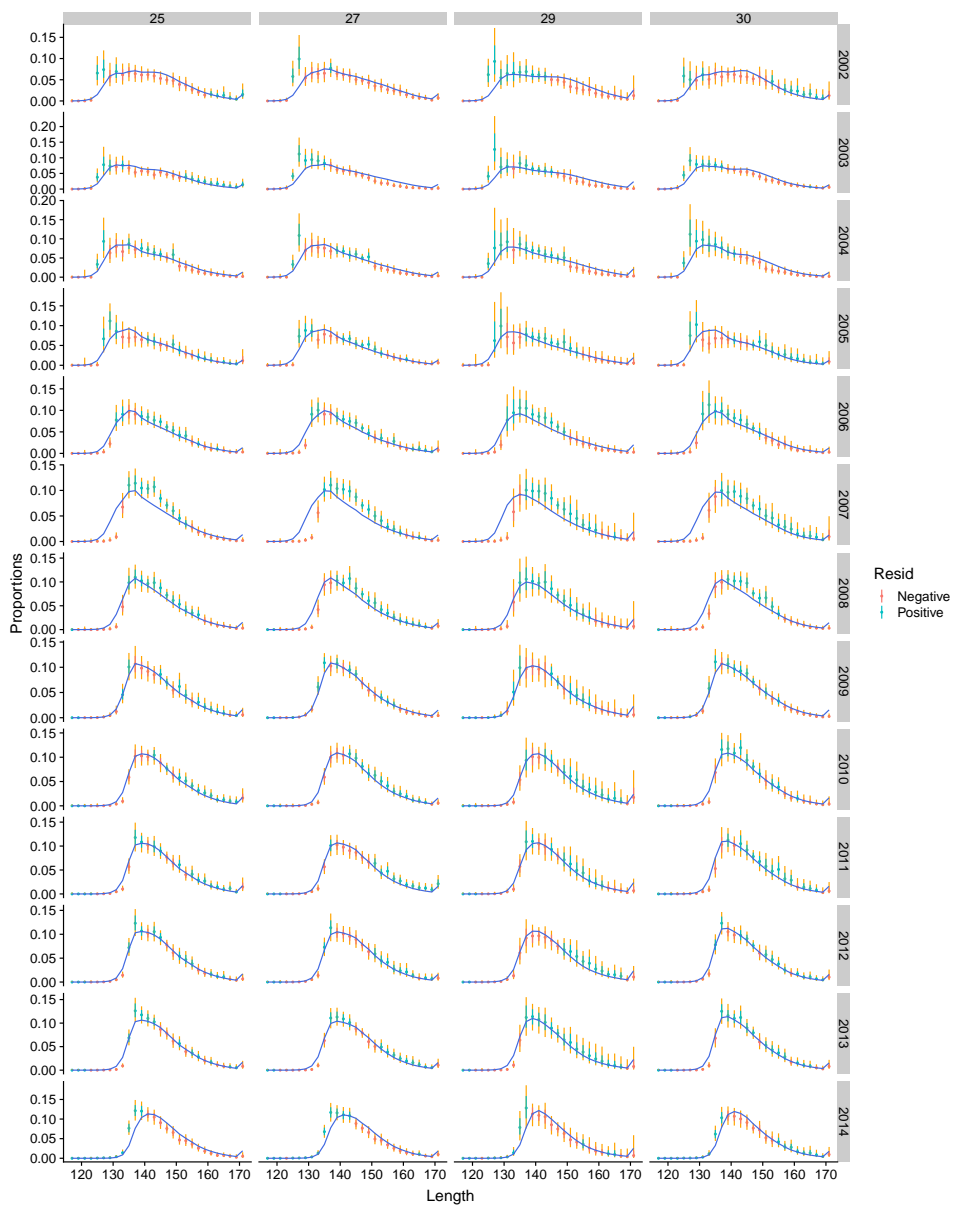


**Figure C-11: Comparison of posterior mean predicted catch sampling length frequency (CSLF) with estimated CSLF proportions and observation error for the spatial stock assessment model for pāua in quota management area PAU 5B. Length classes with positive residuals in blue, with negative residuals in red.**

## C.2 PAU 5D

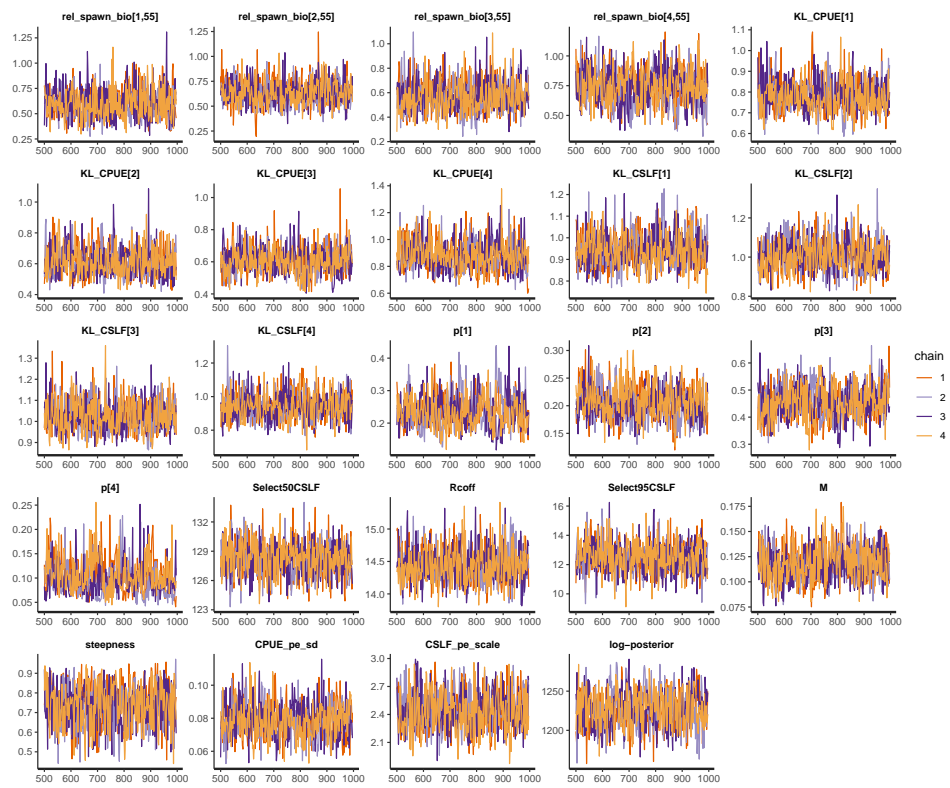


**Figure C-12: Markov chain Monte Carlo (MCMC) trace plots for key model parameters of the spatial stock assessment model for pāua in quota management area PAU 5D (blue); priors are shown as red line where applicable.**

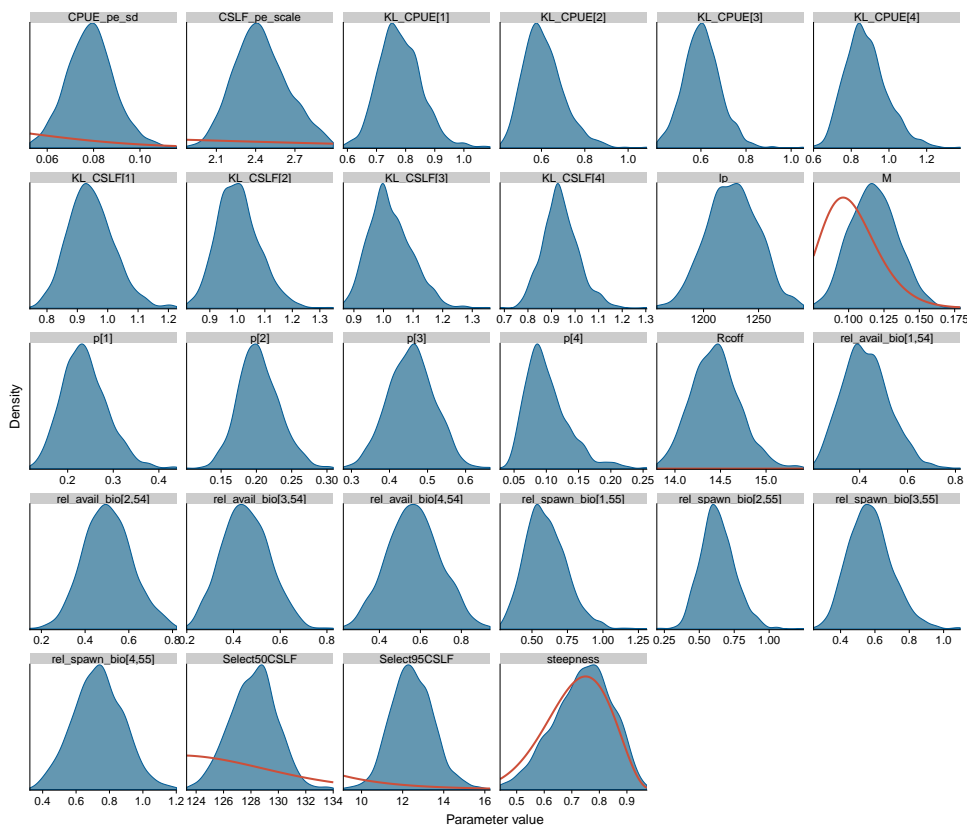


**Figure C-13: Marginal posterior densities for key model parameters of the spatial stock assessment model for pāua in quota management area PAU 5D (blue); priors are shown as red line where applicable.**

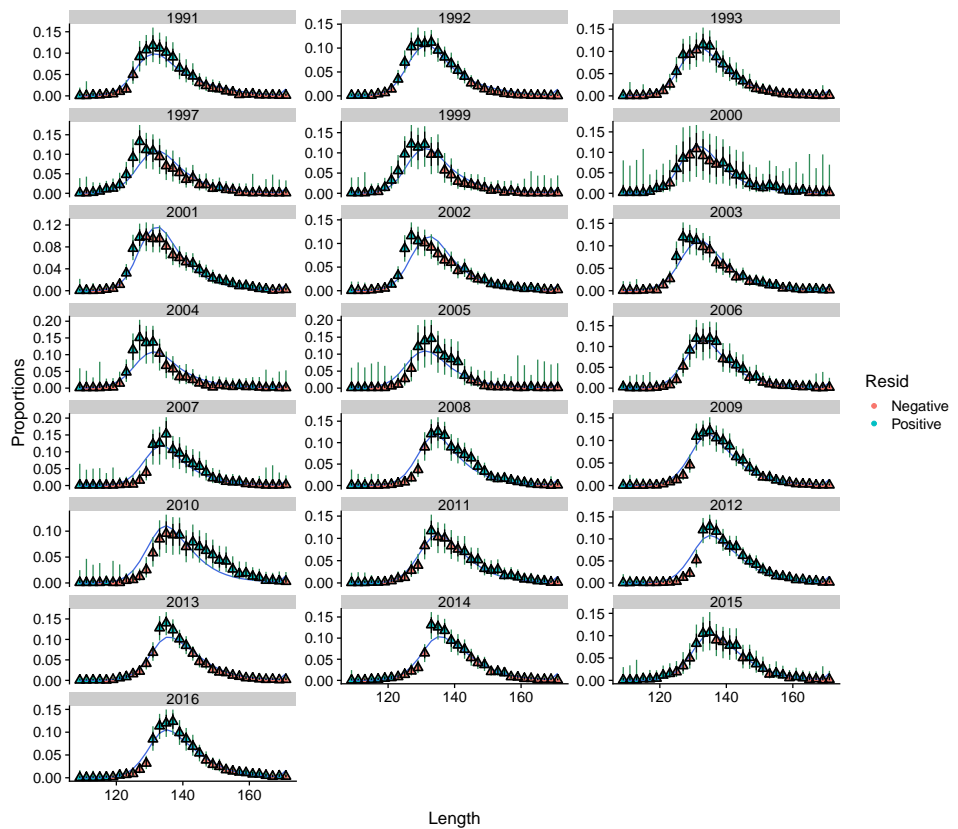


**Figure C-14: Comparison of posterior mean predicted catch sampling length frequency (CSLF) with estimated CSLF proportions and observation error for the single area stock assessment model for pāua in quota management area PAU 5D. Length classes with positive residuals in blue, with negative residuals in red.**

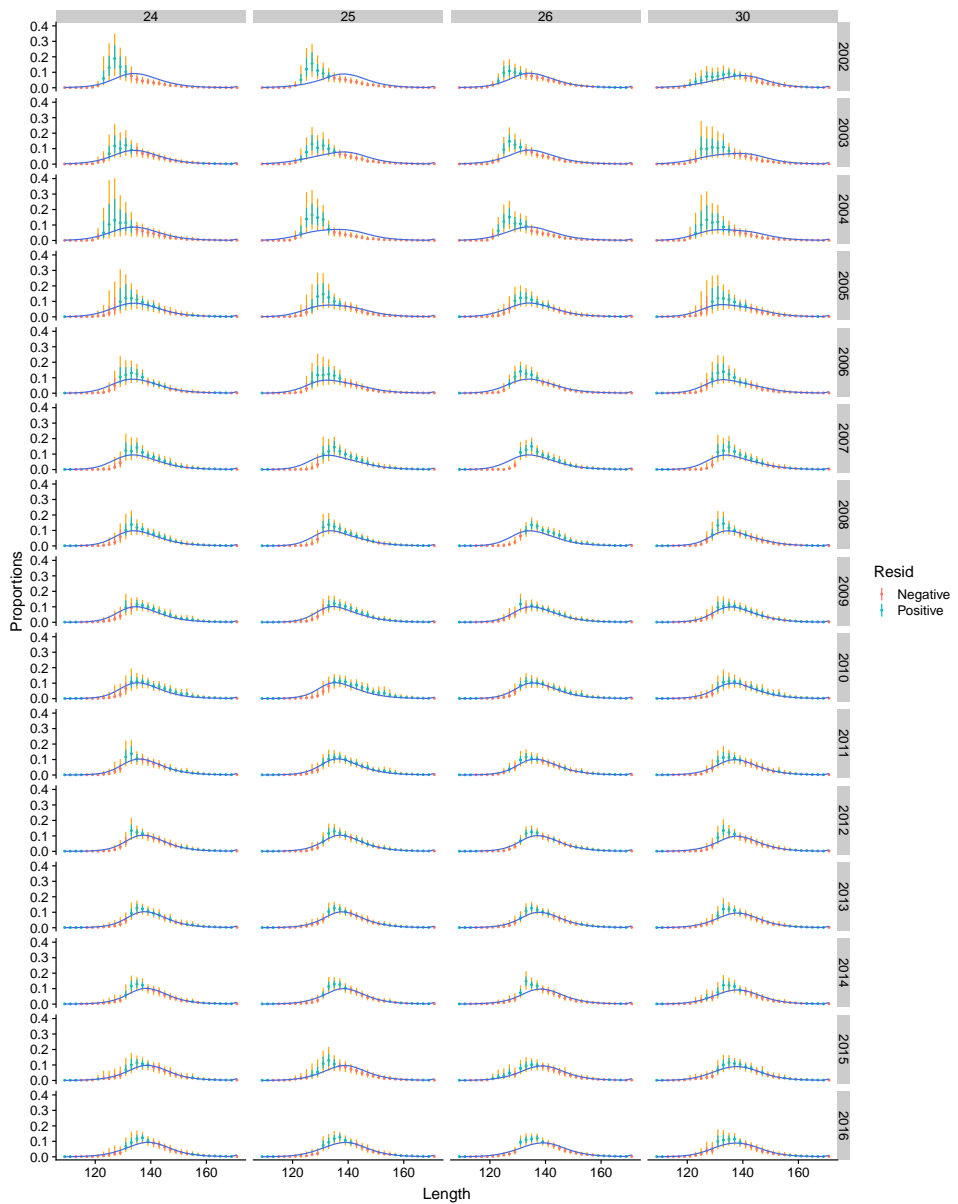


**Figure C-15: Comparison of posterior mean predicted catch sampling length frequency (CSLF) with estimated CSLF proportions and observation error for the spatial stock assessment model for pāua in quota management area PAU 5D. Length classes with positive residuals in blue, with negative residuals in red.**